Geosciences Journal
Vol. 16, No. 4, p. 357 − 379, December 2012
DOI 10.1007/s12303-012-0040-5
ⓒ The Association of Korean Geoscience Societies and Springer 2012

Sequence-stratigraphic comparison of the upper Cambrian Series 3 to Furongian succession between the Shandong region, China and the Taebaek area, Korea: high variability of bounding surfaces in an epeiric platform

Jitao Chen†
S.K. Chough*
Jeong-Hyun Lee
} *School of Earth and Environmental Sciences, Seoul National University, Seoul 151-747, Republic of Korea*
Zuozhen Han *College of Geological Science and Engineering, Shandong University of Science and Technology, Qingdao 266510, China*

ABSTRACT: This study focuses on the stratigraphic sequences and the bounding surfaces in the upper Cambrian Series 3 to Furongian Gushan and Chaomidian formations in the Shandong region, China. The bounding surfaces are compared with those of the coeval succession in the Taebaek area, Korea. According to the vertical arrangement of the facies associations and the identification of the bounding surfaces, three stratigraphic sequences are recognized, representing dynamic changes in accommodation versus sedimentation. The bounding surfaces can be traced in the Shandong region for about 6,000 km^2 in area, but cannot be correlated with those of the Taebaek area (eastern margin of the platform, about 1,000 km apart). Surface 1 is characterized by an abrupt facies change from carbonate to shale, representing a distinct drowning surface. The drowning surface is also diagnosed in the Taebaek area but highly diachronous. Surface 2 is a cryptic subaerial unconformity, reflected by an erosion surface, missing of a trilobite biozone (*Prochuangia* Zone), and an abrupt increase in carbon isotope value. It is not identified in the Taebaek area where the *Prochuangia* Zone is present. Surface 3 is a marine flooding surface, indicated by a subtle transition from flat-bedded microbialite to domal microbialite (or grainstone). It may be correlated with that in the Taebaek area, which is, however, represented by an abrupt facies change from sandstone to limestone-shale alternation. The high variability of the sequence-bounding surfaces is indicative of variable regional factors such as topographic relief, carbonate production, siliciclastic input, and hydrodynamic conditions. It suggests that the sequence-bounding surfaces are invalid for a basin-scale correlation, especially in an epeiric carbonate platform.

Key words: stratigraphic sequence, bounding surface, seafloor relief, Cambrian, North China Platform

1. INTRODUCTION

Carbonate platforms in (sub) tropical regions are commonly characterized by high carbonate productivity with strong catch-up and keep-up capability in response to sea-level rise (e.g., Kendall and Schlager, 1981; Schlager, 2005). In contrast to siliciclastic systems, development of a stratigraphic sequence, a succession of strata deposited during a full cycle of change in accommodation or sediment supply (Catuneanu et al., 2009), on carbonate platforms depends largely on the complex interaction among eustatic changes, regional tectonics, types of carbonate production, and environmental conditions (Schlager, 1993; Pomar, 2001; Brandano and Corda, 2002; Caron et al., 2004; Mateu-Vicens et al., 2008; Pomar and Kendall, 2008; Catuneanu et al., 2009). Growth potential of carbonate factories often causes uneven topographic relief of various scale (Kendall and Schlager, 1981; Burchette and Wright, 1992; Schlager, 1993; Burgess, 2001; Pomar, 2001; Bádenas and Aurell, 2008; Woo, 2009), affecting the stacking patterns of strata and the formation of sequence-stratigraphic surfaces.

High-frequency (e.g., third- or higher-order, <10 m.y. in duration) stratigraphic sequences often formed in carbonate platforms with lateral variability of their bounding surfaces (e.g., Strasser et al., 1999; Brett et al., 2011). Topographic relief of the bounding surfaces can be represented by either subaerial-exposure features or subtle changes in sedimentary facies (e.g., Schlager, 1989; Adams and Grotzinger, 1996; Jiang et al., 2002). There are, however, a number of questions with regard to the formation and variability of the bounding surfaces. Do the bounding surfaces form synchronously during base-level changes? What controls the formation of the bounding surfaces during long-term rise in sea level? Can the bounding surfaces be traced across the entire platform and useful for basin-scale correlation, especially in the vast epeiric platform?

This study focuses on the variability of bounding surfaces of certain stratigraphic units in the North China Platform, i.e., the upper Cambrian Series 3 to Furongian Gushan and Chaomidian formations. The succession (ca. 350 m in thickness) in Shandong Province (mideast of the platform) consists mainly of various shallow-marine carbonates with minor shale layers that are generally characterized by a facies transition from limestone-shale/marlstone alternation to coarse-grained carbonate sediments, largely indicative of long-term

*Corresponding author: sedlab@snu.ac.kr
†Present address: Nanjing Institute of Geology and Palaeontology, Chinese Academy of Sciences, Nanjing 210008, China

sea-level rise superimposed by high-frequency sea-level fluctuations (Meng et al., 1997). However, there are certain features that make it difficult for large-scale correlation (with the Taebaek area, Korea) by bounding surfaces across the epeiric platform. The primary aims of this paper are to diagnose the bounding surfaces of high-frequency stratigraphic sequences in a carbonate platform and to evaluate the variability of the bounding surfaces in sequence-stratigraphic perspectives.

2. GEOLOGICAL SETTING

The North China Platform, an epeiric platform, developed on the Sino-Korean Block (SKB) in (sub) tropical regions (Scotese and McKerrow, 1990; Meng et al., 1997; Kwon et al., 2006; Chough et al., 2010; McKenzie et al., 2011) (Fig. 1). It covers an area of 1,500 km east-west and 1,000 km north-south (Meng et al., 1997) (Fig. 1a). It is bounded to the north by a major fault and suture zone, the Hinggan fold belt. The Qinling-Dabieshan fold belt demarcates the southern margin of the platform against the South China Block (SCB). The Tanlu fault in the east formed during collision of the SKB and the SCB in the Early Triassic (Chough et al., 2000). The western boundary of the platform is characterized by a thick sequence of platform-margin and deep-basinal sediments. According to the tectonic reconstruction and stratigraphic correlation of the Paleozoic basins, both the Pyeongnam Basin (North Korea) and the Taebaeksan Basin (South Korea) comprise the eastern margin of the platform (Chough et al., 2000; Choi and Chough, 2005) (Fig. 1).

Sedimentation on the North China Platform started in the Cambrian Epoch 2 and continued until the Middle to Late Ordovician when the entire platform was subaerially exposed, forming a thick (ca. 1,800 m in thickness) succession of mixed carbonate and siliciclastic sediments (Meyerhoff et al., 1991; Meng et al., 1997). The entire succession represents a long-term transgression of a second-order sea-level rise that lasted for about 70 m.y. (Meng et al., 1997). After a platform-wide hiatus during the middle Paleozoic (Late Ordovician to Early Carboniferous), coal-bearing, shallow marine and continental deposits accumulated on the platform. Deposition was terminated in the Early Triassic by the regional uplift that resulted from the collision between the SKB and the SCB (Lee and Chough, 2006).

The Cambrian strata are superbly exposed in Shandong Province (mideast of the North China Platform) (Fig. 1). The strata yield abundant and diverse fossils such as trilobites, gastropods, brachiopods, cephalopods, and echinoderms. Twenty-one trilobite biozones have been identified in the Cambrian succession (Chough et al., 2010). The Cambrian succession in Shandong Province consists of 6 lithostratigraphic units (Liguan, Zhushadong, Mantou, Zhangxia, Gushan, and Chaomidian formations in ascending order), unconformably overlying Precambrian granitic gneiss or metasedimentary

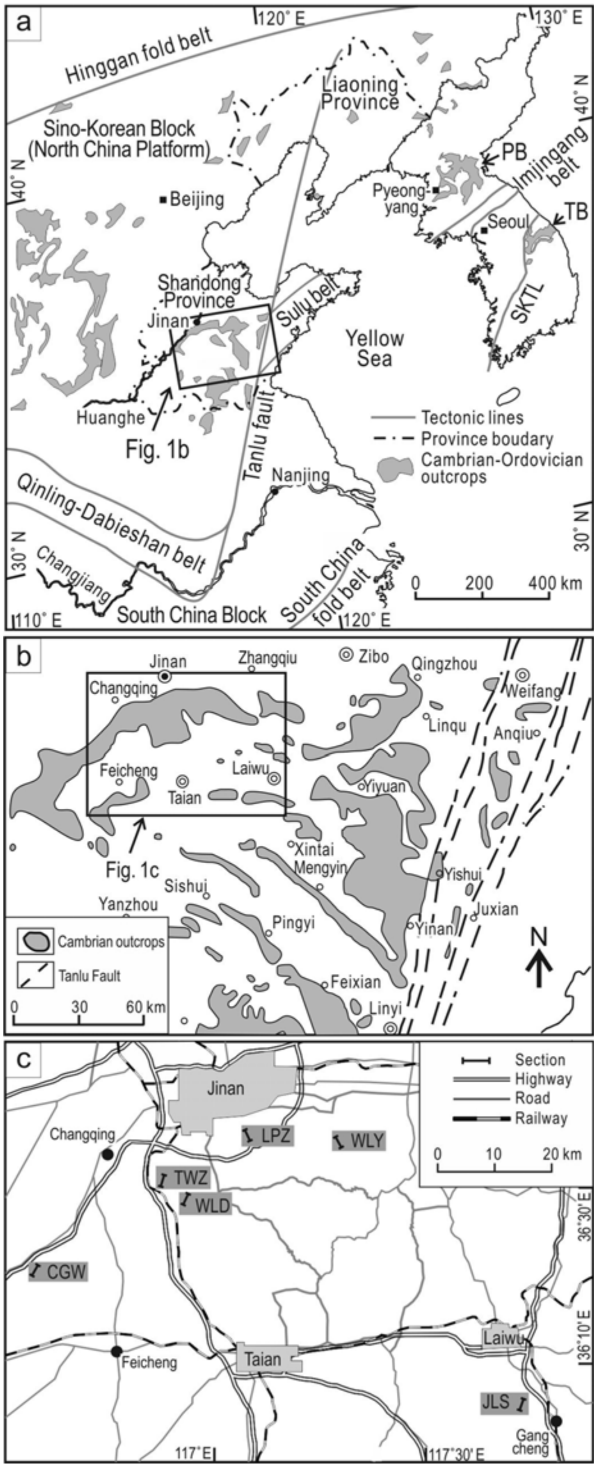

Fig. 1. Simplified geologic map and location of the study area. (a) Tectonic boundaries and distribution of the Cambrian-Ordovician outcrops of the North China Platform (modified after Kwon et al., 2006). PB: Pyeongnam Basin. TB: Taebaeksan Basin, SKTL: South Korean Tectonic Line. (b) Distribution of the Cambrian outcrops in Shandong Province (modified after Zhang et al., 1994). (c) Location of the measured sections. CGW: Chengouwan section, TWZ: Tangwangzhai section, WLD: Wanglaoding section, LPZ: Laopozhuang section, WLY: Wanliangyu section, JLS: Jiulongshan section.

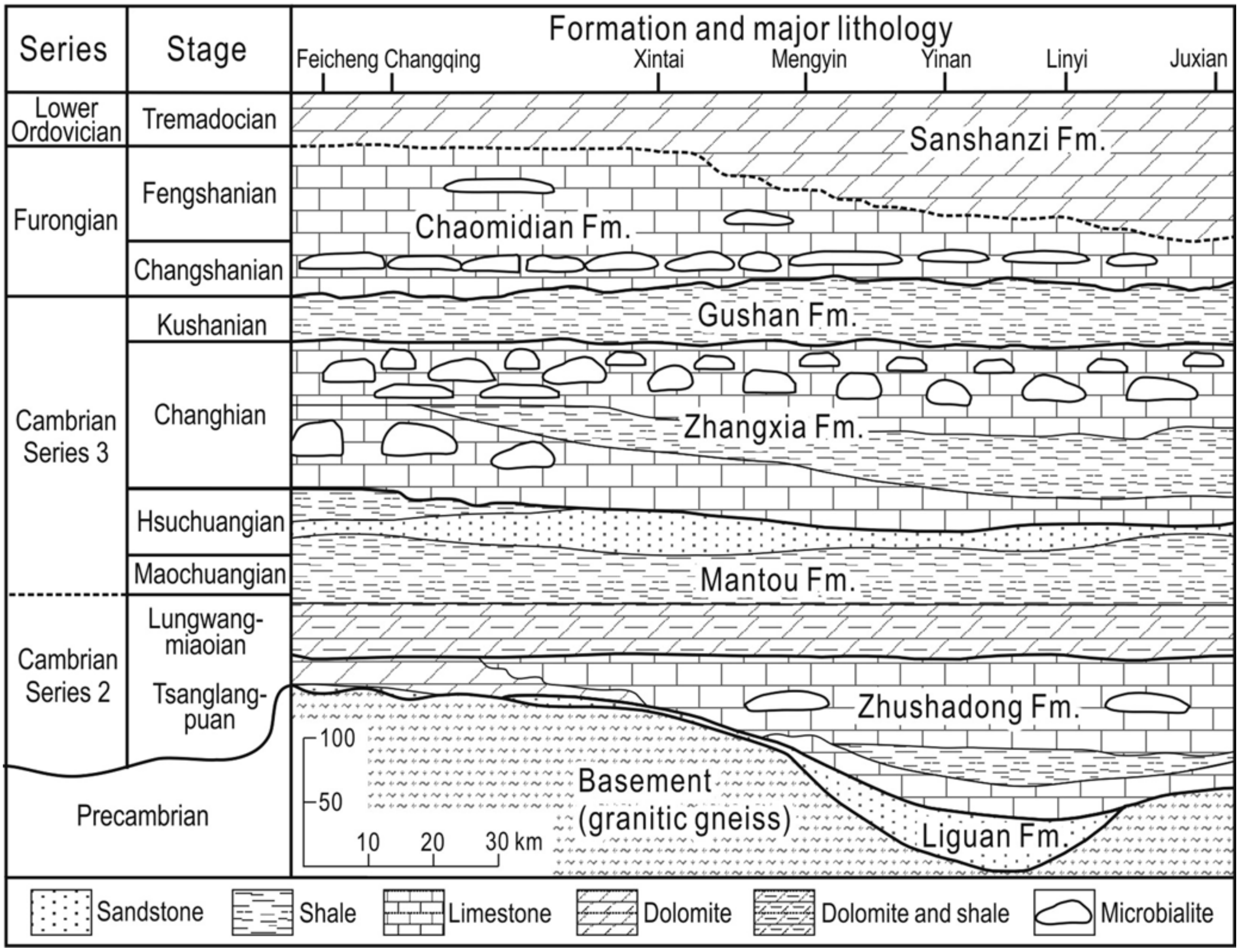

Fig. 2. Spatio-temporal distribution of the Cambrian succession in Shandong Province (modified after Zhang et al., 1994). For location, see Figure 1b.

rocks and conformably underlying Ordovician dolostones and limestones (Fig. 2).

The basal Liguan Formation (laterally discontinuous, 0–30 m thick) consists mainly of quartzose sandstone and mudstone (Fig. 2). The overlying Zhushadong Formation (15–40 m thick) is dominated by stromatolitic and dolomitic lime mudstone, and locally bioturbated wackestone. The Mantou Formation (ca. 250 m thick) consists of mixed siliciclastic and carbonate sediments including purple mudstone, sandstone, and various carbonates. The overlying Zhangxia Formation (ca. 180 m thick) is characterized by a variety of microbialites and carbonates, and locally shaly sediments. The Gushan Formation (52–105 m thick) comprises shale-dominated facies and formed during the late Cambrian Epoch 3 Kushanian Age (*Blackwelderia* and *Neodrepanura* zones) (Fig. 3). The overlying Chaomidian Formation (190–260 m thick) is dominated by various carbonate facies, and formed during the Furongian including the Changshanian Age (*Chuangia*, *Changshania-Irvingella*, and *Kaolishania* zones) and Fengshanian Age (*Asioptychaspis-Tsinania*, *Quadraticephalus*, and *Mictosaukia* zones) (Fig. 3).

3. MATERIALS AND METHODS

Three complete sections (Tangwangzhai, Laopozhuang, and Jiulongshan sections) and three complementary sections (Chengouwan, Wanliangyu, and Wanglaoding sections) (ca. 1,100 m in total thickness) have been measured (scale of 1:10 or 1:50) in well-exposed outcrops in Shandong Province, China (Figs. 1c and 4). Sedimentary facies of the Gushan and Chaomidian formations are classified and described based mainly on lithology (composition and grain size) and sedimentary structures as well as texture and bed geometry (Table 1). The facies are described largely according to the classification scheme of Dunham (1962). Common descriptive facies names such as limestone-shale/marlstone alternation, limestone breccia and conglomerate, and various microbialites (e.g., stromatolite) are used. Sketch and line

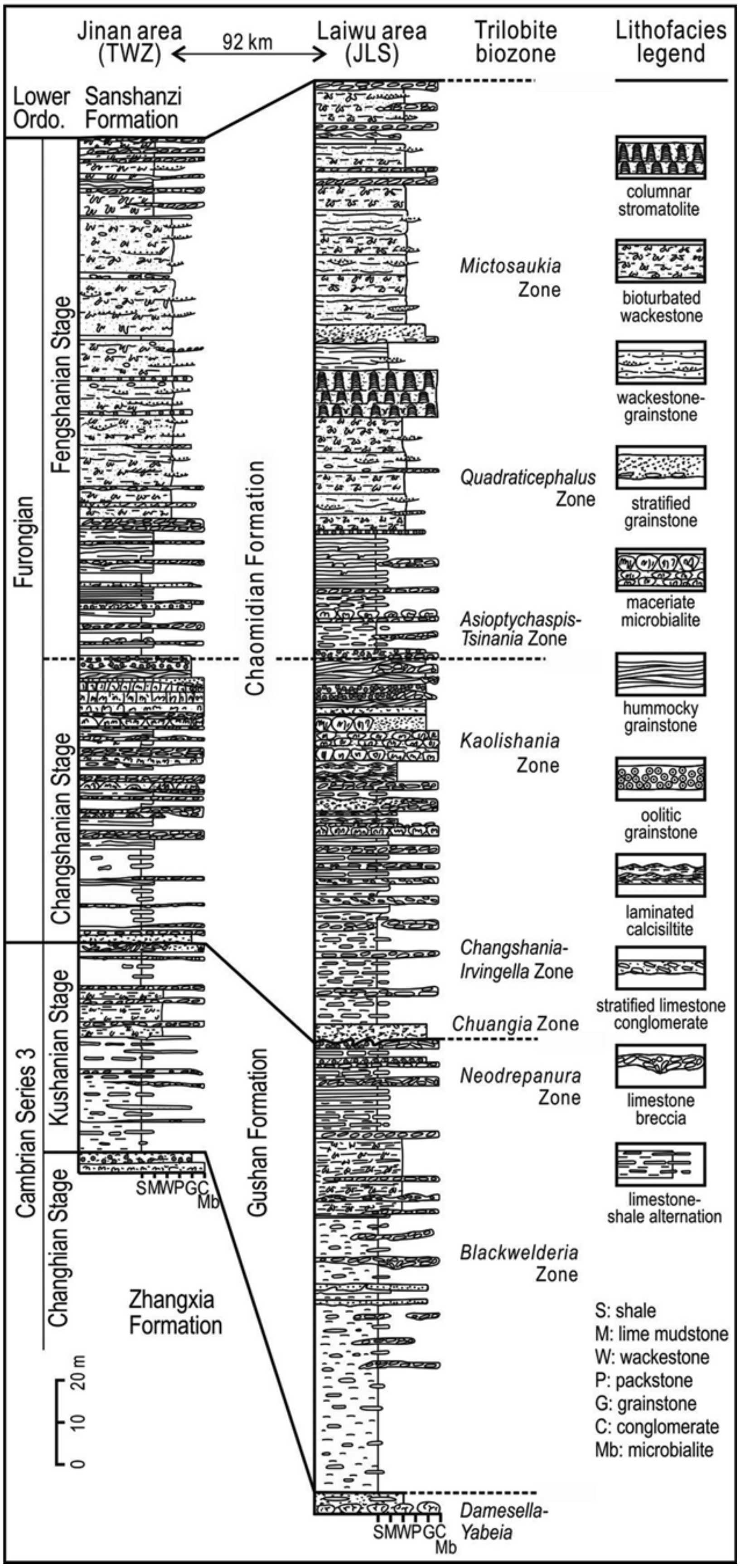

Fig. 3. Schematic sedimentary logs of the Gushan and Chaomidian formations in the Jinan and Laiwu areas. For location, see Figure 1c.

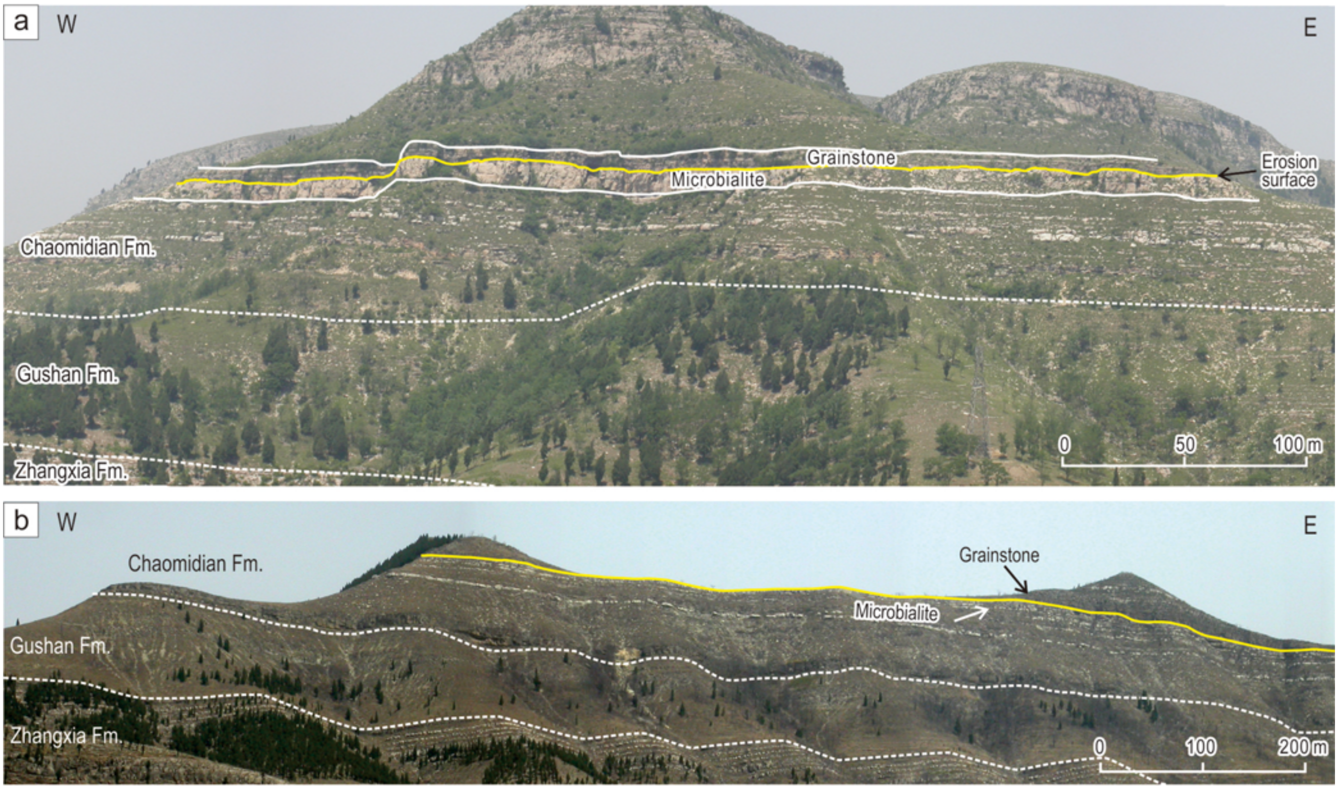

Fig. 4. Representative outcrop sections, showing laterally traceable lithofacies units. (a) Tangwangzhai section. (b) Jiulongshan section. The Zhangxia Formation is dominated by various carbonates. The overlying Gushan and Chaomidian formations are characterized by a gradual transition from shale-dominated facies to carbonate-dominated facies. An extensive microbialite bed, overlain by grainstones, occurs in the middle part of the Chaomidian Formation.

drawings portray sedimentary structures and texture. Slabs of sampled specimens (polished and etched) illustrate cryptic sedimentary structures. Over 400 thin sections have been observed under microscope for compositional and microfacies analyses.

4. SEDIMENTARY FACIES

Eighteen sedimentary facies are identified in the Gushan and Chaomidian formations (Table 1; Figs. 5 and 6), which comprise 5 facies associations (FAs) (Chen et al., 2011) (Table 2; Figs. 6 and 7). The facies association units are correlated among the measured sections, which represent various shallow-marine settings (Table 2; Fig. 7). FA1 is dominated by shale and limestone (limestone-shale/marlstone alternation, calcarenite, and limestone breccia), representing a deep-subtidal setting. FA2 consists mainly of thin-bedded lime mudstone intercalated with shale or marlstone, laminated calcisiltite, and limestone breccia and conglomerate, as well as a few beds of stratified grainstone and microbialite, which represents a relatively shallow-subtidal setting. FA3 mainly comprises various grainstones (normally graded, crudely wavy-stratified, and planar, trough, and hummocky cross-stratified) with a minor portion of limestone-shale/marlstone alternation, and limestone conglomerate and breccia, indicating a generally high-energy, storm-dominated shore/shoal setting. FA4 is dominated by biostromal, thick-bedded microbialite (including tabular maceriate, columnar maceriate, and columnar chaotic microbialite), reflecting an extensive subtidal microbial flat. FA5 is characterized by a thick monotonous succession of mainly bioturbated lime mudstone to wackestone and wacke- to grainstone with sporadic stromatolite, representing a restricted platform interior.

5. STRATIGRAPHIC SEQUENCES AND BOUNDING SURFACES

According to the vertical arrangement of the facies associations and the identification of the physical surfaces, three stratigraphic sequences (approximately 2–5 m.y. in duration) can be established in the Gushan and Chaomidian formations (Fig. 7). The three sequences are bounded at the base by a drowning surface (surface 1) (Fig. 8), a subaerial unconformity (surface 2) (Figs. 9 and 10), and a marine flooding surface (surface 3) (Figs. 11 and 12), respectively. These bounding surfaces are well traced in all measured sections for about 6,000 km^2 in area in Shandong Province (Fig. 7).

Table 1. Sedimentary facies in the Gushan and Chaomidian formations

Sedimentary facies	Description	Interpretation
Shale (facies Sh)	Greenish-gray (yellowish-gray and partly dark purple) shale (Fig. 5a); mainly composed of quartz and clay minerals, and some calcite and dolomite; intercalated with calcareous nodules or irregular concretions; usually fissile and papery, partly calcareous.	Low-energy subtidal deposits most likely below storm wave base.
Limestone-shale alternation (facies L-S)	Alternation of planar to nodular limestone and greenish-gray shale (Fig. 5a); limestone composed of micrite; shale composed mainly of argillaceous materials (quartz and clay minerals, 81%), and small fractions of calcite and dolomite (19%); sporadic horizontal burrows; well-preserved trilobite fossils (e.g., *Blackwelderia* and *Neodrepanura*) on bedding plane.	Low-energy subtidal deposit below fair-weather wave base.
Limestone- marlstone alternation (facies L-M)	Alternation of limestone and marlstone layers; about 1 cm in thickness; limestone composed of micrite with trilobite fragments (5–20%); marlstone composed of dolomite (16.11%), calcite (53.93%), and argillaceous materials (29.96%); slightly bioturbated with sporadic horizontal or inclined burrows; lenses of bioclasts intercalated in some horizons.	Low-energy subtidal deposit below fair-weather wave base.
Thin-bedded lime mudstone (facies Ltb)	Slightly bioturbated thin-bedded lime mudstone (Fig. 5b); lime mudstone composed of micrite and small fractions of bioclasts; sporadic horizontal to inclined burrows; commonly overlying L-S or L-M with gradational boundary, forming decimeter- to meter-scale units.	Low-energy subtidal deposit modified by bioturbation.
Laminated calcisiltite (facies Cl)	Parallel, ripple, and low-angle cross-laminated calcisiltite intercalated with dolomitic marlstone or shale (Fig. 5b); composed of silt-sized calcite particles; wavy-bedded, unidirectional and low-angle cross-lamination with internal truncation boundary; climbing ripples; partly bioturbated with burrows.	Subtidal deposits by unidirectional currents (partly combined with waves).
Bioturbated wackestone (facies Wb)	Moderately to severely bioturbated (ichnofossil index-3 to -4) (Fig. 5c); horizontal to inclined burrows; mottled texture; composed mainly of micrite, fossil fragments, and peloids; partly intercalated with thin bioclastic grainstone with sharp lower boundary.	Low-energy subtidal deposits modified by bioturbation.
Wackestone to grainstone (facies W-G)	Flaser-bedded wackestone often separated by shale partings; slightly bioturbated; often intercalated with lenses or thin layers of grainstone with sharp lower boundary (Fig. 5d); grainstone commonly massive, normally graded, or planar and cross-stratified; abundant and variable fossil fragments such as cephalopods, bivalves, gastropods, trilobites, algae, and echinoderms.	Low-energy subtidal deposits with intermittent higher energy deposits.
Hummocky and swaley cross-stratified grainstone (facies Ghsc)	Peloidal grainstone, composed of coarse silt- to very fine sand-size peloids and small fraction of fossil fragments; each unit either laterally continuous or discontinuous, varying in thickness from a few dm to 2 m; thick beds amalgamated with internal sharp boundaries (Fig. 5e); *Skolithos*, 1–5 cm in depth; variation in thickness of laminae.	Storm-induced combined flows, above storm wave base.
Planar and trough cross-stratified grainstone (facies Gptc)	Oolitic and bioclastic grainstones (Fig. 5f); planar and trough cross-stratified; oolitic grainstone dominantly composed of ooids, whereas bioclastic grainstone composed of fragments of fossils (trilobites, brachiopods, algae, and echinoderms), often with glauconite grains and intraclasts; asymmetrical mega-ripple bed forms (ripple height 10 cm and length about 100 cm).	Migration of subaqueous 2D or 3D dune of carbonate sands.
Crudely wavy-stratified grainstone (facies Gcw)	Oolites and bioclastic grainstones; symmetric (mega) ripples (ripple height 8 cm and length about 60 cm) on the top of oolite beds; oolites composed of ooids (>50%), peloids, and fossil fragments (Fig. 5g), whereas bioclastic grainstones composed of various fossil fragments (trilobites and brachiopods); abundant glauconite grains.	High-energy wave deposition on shoal or shoreface settings.
Normally graded grainstone (facies Gng)	Massive or normally graded pack- to grainstone (Fig. 5h), mainly composed of fossil fragments (trilobites, brachiopods, algae, echinoderms, and cephalopods; a few mm up to 10 mm in length), peloids, and ooids (0.2–0.5 mm in diameter); subangular, granule- to pebble-size intraclasts of lime mudstone to grainstone as well as microbialite.	Moderately agitated shallow-subtidal deposits.
Calcarenite (facies CA)	Calcarenite containing a few clasts of lime mudstone; composed of packstone to grainstone with elongate trilobite fragments; crudely laminated or normally graded; overlying lime mudstone with irregular sharp boundaries, showing load and flame structures.	Deposition from dilute density (turbidity) currents.
Limestone conglomerate (facies LC)	Polymictic clasts of lime mudstone, wacke- to packstone, grainstone, and sometimes microbialite and conglomerate, and grainstone matrix (Fig. 5i); poorly to moderately sorted clasts, varying in grain size from granule to pebble, with dominantly subrounded to rounded corners; clasts usually flat-lying or imbricated (Fig. 5i); either clast-supported or matrix-supported, and crudely cross-stratified; sharp irregular lower boundary and either sharp or gradational upper boundaries.	Deposits by strong currents or waves, most likely induced by storms.
Limestone breccia (facies LB)	Monomictic to oligomictic clasts in a matrix of marlstone and/or grainstone (Fig. 5j); flat to irregular, sheet-, disc-, or blade-shaped clasts; random clast positions (intact, inclined, vertical, and disorganized); transitional boundaries from underlying bed; laterally discontinuous; often accompanied by soft-sediment deformation structures.	Soft-sediment deformation during early diagenesis.
Columnar stromatolite facies (facies Sc)	Centimeter- to meter-scale columnar-shaped (Fig. 5k); bioclastic grainstone and bioturbated wackestone between columns; composed of micritic *Girvanella* colonies, peloids, fragments of fossils (trilobites, algae, cephalopods, and gastropods), and partly intraclasts.	High-energy subtidal deposits with occasional lower-energy deposits.

Table 1. (continued)

Sedimentary facies	Description	Interpretation
Calcarenite (facies CA)	Calcarenite containing a few clasts of lime mudstone; composed of packstone to grainstone with elongate trilobite fragments; crudely laminated or normally graded; overlying lime mudstone with irregular sharp boundaries, showing load and flame structures.	Deposition from dilute density (turbidity) currents.
Limestone conglomerate (facies LC)	Polymictic clasts of lime mudstone, wacke- to packstone, grainstone, and sometimes microbialite and conglomerate, and grainstone matrix (Fig. 5i); poorly to moderately sorted clasts, varying in grain size from granule to pebble, with dominantly subrounded to rounded corners; clasts usually flat-lying or imbricated (Fig. 5i); either clast-supported or matrix-supported, and crudely cross-stratified; sharp irregular lower boundary and either sharp or gradational upper boundaries.	Deposits by strong currents or waves, most likely induced by storms.
Limestone breccia (facies LB)	Monomictic to oligomictic clasts in a matrix of marlstone and/or grainstone (Fig. 5j); flat to irregular, sheet-, disc-, or blade-shaped clasts; random clast positions (intact, inclined, vertical, and disorganized); transitional boundaries from underlying bed; laterally discontinuous; often accompanied by soft-sediment deformation structures.	Soft-sediment deformation during early diagenesis.
Columnar stromatolite facies (facies Sc)	Centimeter- to meter-scale columnar-shaped (Fig. 5k); bioclastic grainstone and bioturbated wackestone between columns; composed of micritic *Girvanella* colonies, peloids, fragments of fossils (trilobites, algae, cephalopods, and gastropods), and partly intraclasts.	High-energy subtidal deposits with occasional lower-energy deposits.
Tabular maceriate microbialite (facies Mtm)	Centimeter- to decimeter-scale branching and converging structures in vertical sections, and irregular circles or rambling maze-like structures in bedding surfaces (i.e., maceria structures); chaotic internal structures of maceriae; intermacerial sediment mainly composed of lime mud and a few trilobite fragments, whereas maceriae composed of micrite and calcified *Girvanella* as well as *Renalcis*-like microbe colonies (1–10 mm in size); often forming laterally traceable mounds (ca. 1–2 m thick and ~10 m wide).	Relatively low-energy deposits below normal wave base.
Columnar maceriate microbialite (facies Mcm)	Large columns (>60 cm in diameter) of maceriate microbialites; internal part of the columns dominated by maceriae, with chaotic outer rim (a few cm in thickness) (Fig. 5l); coarse-grained sediments such as intraclasts, peloids, and bioclasts present between columns; often gradually changing upward to columnar chaotic microbialite (facies Mcc), accompanied by a decrease in amounts of maceriae, an increase in amounts of intercolumnar grainstones, and a decrease in column diameter.	Intermediate-energy deposits near normal wave base.
Columnar chaotic microbialite (facies Mcc)	Columnar microbialites (10–15 cm in diameter) with generally chaotic internal structures; elongation aspect ratio (i.e., ratio of height to width) of columns ranges from 3:1 to 10:1; composed mainly of calcified *Girvanella* and *Renalcis*-like microbes with peloids and bioclasts; crudely stratified grainstones among the microbialite columns; abundant bivalves locally concentrated in both intercolumnar sediments and microbialites.	High-energy shallow-subtidal deposits above normal wave base.

5.1. Bounding Surface 1 and Sequence 1

5.1.1. Description

Bounding surface 1 is characterized by an abrupt change in facies from the underlying carbonate in the Zhangxia Formation to the overlying shale in the Gushan Formation (Fig. 8). The upper part of the Zhangxia Formation consists mainly of thick-bedded oolite and thrombolitic microbialite in the northwest (Tangwangzhai and Laopozhuang sections) (Fig. 8a) and wacke- to packstone, thrombolitic microbialite, and limestone-shale alternation in the southeast (Jiulongshan section) (Fig. 8b). The topmost part of the Zhangxia Formation contains abundant glauconite grains and fossil fragments. Above surface 1, the lower part of the sequence 1 consists dominantly of dark and greenish-gray shale intercalated with nodular and thin-bedded limestone (FA1). In the Jiulongshan section, several calcarenite beds (facies CA) with load and flame structures and sharp bases are intercalated in the shale-dominated facies (Fig. 6). The upper part of the sequence 1 contains more carbonates such as limestone-marlstone alternation, thin-bedded lime mudstone, laminated calcisiltite, cross-stratified limestone conglomerate, and a few grainstone beds (FA2) (Fig. 7). The topmost part of the sequence 1 consists of an extensive, strongly deformed limestone bed (containing bioclastic wacke- to packstone, oolitic grainstone, and thin-bedded lime mudstone). It is characterized by various soft-sediment deformation structures such as limestone breccia, chaotic laminae, homogenized oolites, and carbonate dykes.

5.1.2. Interpretation

Surface 1 represents drowning of carbonate factories. It is indicated by an abrupt facies shift from shallow-water carbonates to deep-water siliciclastics (*sensu* Schlager, 1989, 1999). Surface 1 formed by drowning of the microbialite-dominated carbonate factories (Zhangxia Formation) with rapid rise in base level (Fig. 13a). Under deepened waters, carbonate production was shut down and the increase in rate of accommodation became higher than that of sediment supply, resulting in sediment starvation. Sedimentation dur-

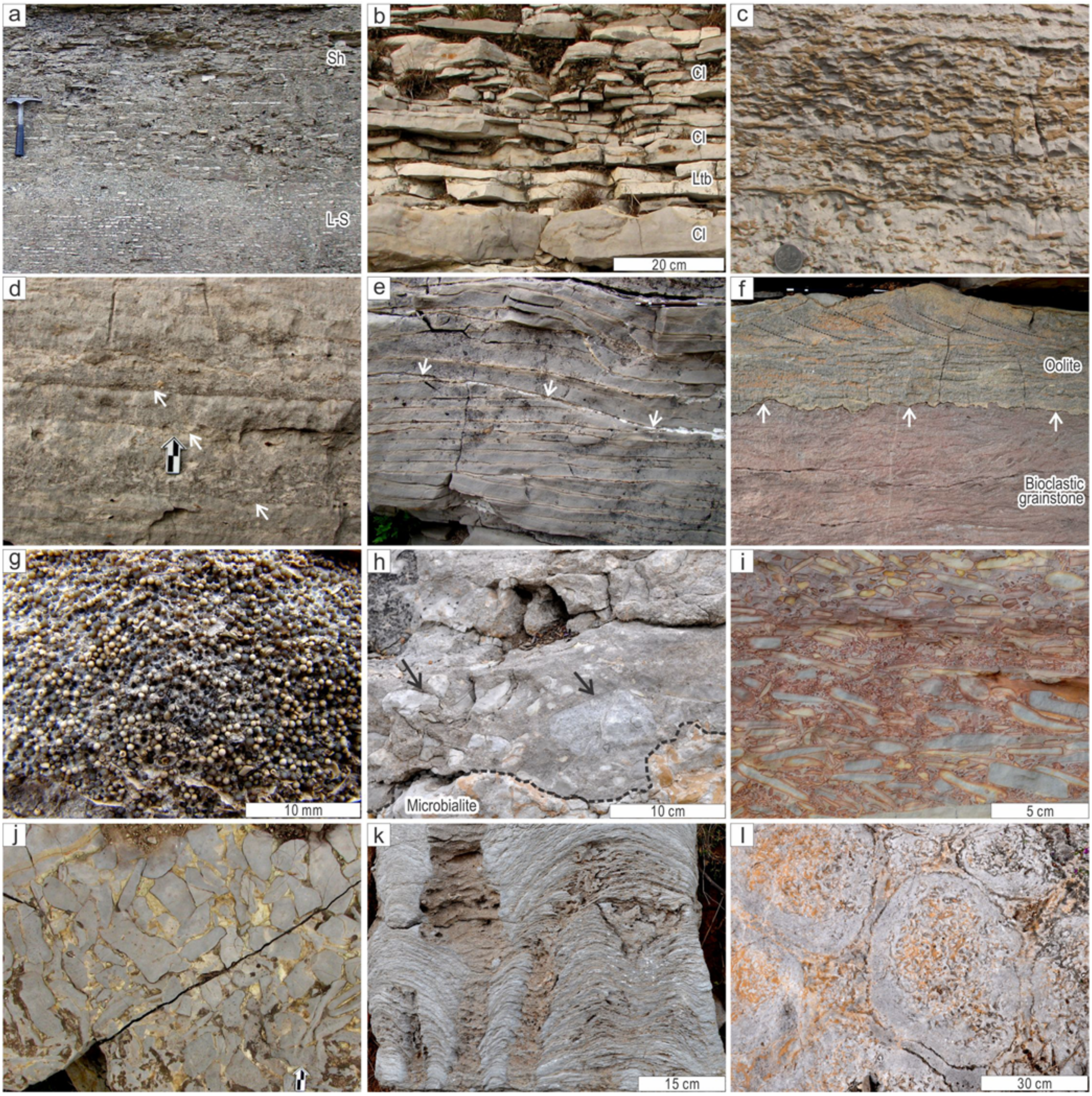

Fig. 5. Sedimentary facies. (a) Greenish gray shale (facies Sh) and limestone-shale alternation (facies L-S). Hammer is 28 cm long. (b) Ripple or low-angle cross-laminated calcisiltite (facies Cl) intercalated with thin-bedded lime mudstone (facies Ltb). (c) Bioturbated wackestone (facies Wb) with mottled texture (ichnofossil index-3). Coin is 25 mm in diameter. (d) Wackestone with discontinuous layers of grainstone and conglomerate (arrows) (facies W-G). Scale bar is 2 cm long. (e) Hummocky and swaley cross-stratified grainstone (facies Ghsc) with internal truncation (arrows). Pencil is 14.5 cm long. (f) Planar to trough cross-stratified grainstone (facies Gptc) with ripple marks at the top. The boundary between oolite and bioclastic grainstone is characterized by stylolite (arrows). Pencil is 14.5 cm long. (g) Crudely wavy-stratified oolitic grainstone (facies Gcw), partly containing chertified ooids. (h) Normally graded gravelly grainstone (facies Gng) with microbialite debris (arrows) in the lower part. Dash line indicates the irregular boundary overlying the microbialite. (i) Limestone conglomerate (facies LC) with imbricated, polymictic clasts and grainstone matrix. (j) Plan view of limestone breccia (facies LB), showing progressive deformation from intrastratal fragmentation to slight mobilization and total disruption (from upper left to lower right). Scale bar is 2 cm long. (k) Columnar stromatolite (facies Sc). Space between columns is filled with gravelly grainstone. (l) Plan view of columnar maceriate microbialite (facies Mcm) with chaotic outer rim and maceriate core.

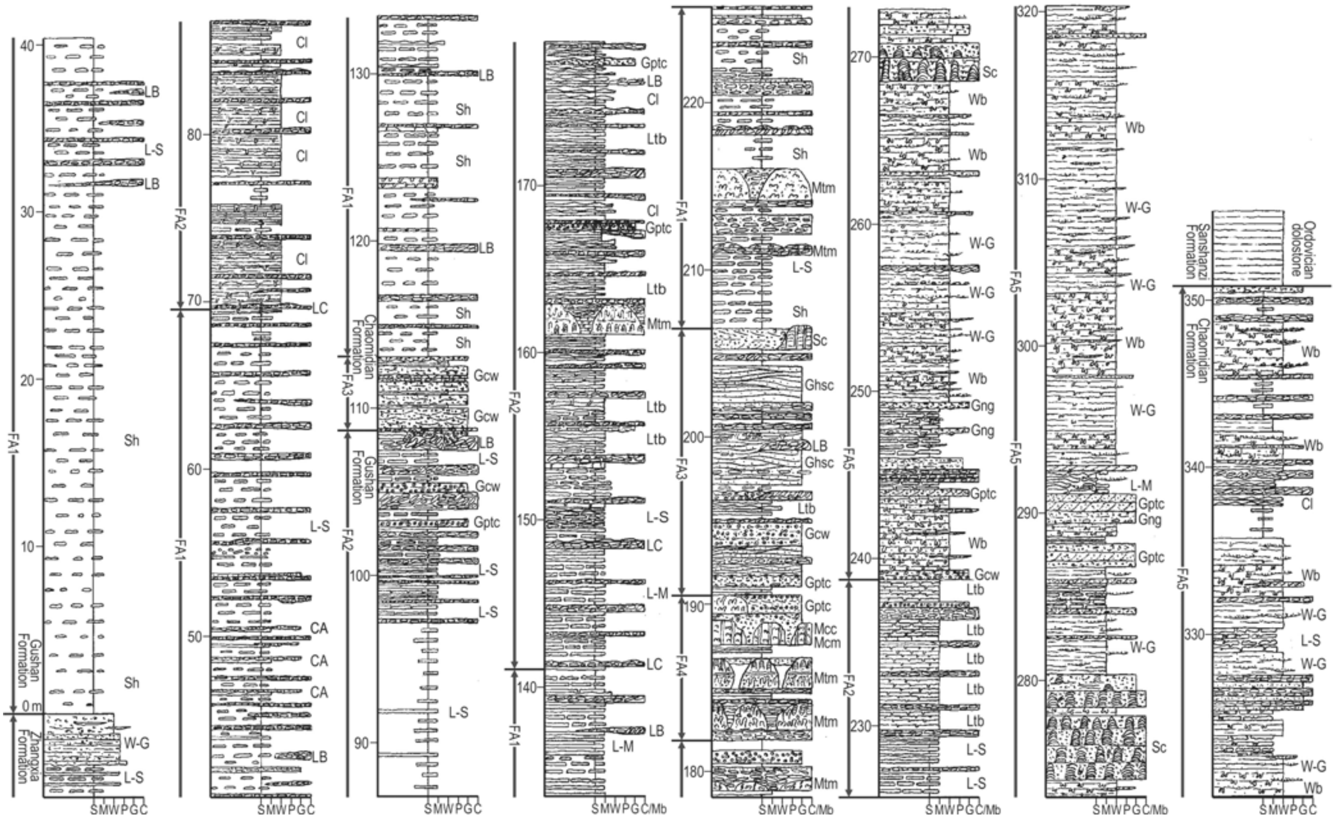

Fig. 6. Representative sedimentary log of the Gushan and Chaomidian formations in the Jiulongshan section (for location, see Fig. 1c; for facies code, see Table 1). S: shale, M: lime mudstone, W: wackestone, P: packstone, G: grainstone, C: limestone conglomerate, Mb: microbialite. FA1: shale-dominated facies association; FA2: thin-bedded limestone facies association; FA3: grainstone facies association; FA4: microbialite facies association; FA5: wackestone to grainstone facies association.

ing this period was largely due to suspension settling of terrigenous fines (FA1). After drowning of the carbonate factories, however, the successive sedimentation was affected by the inherited topographic variations of the Zhangxia platform (i.e., ooid shoal and microbial platform in the northwest, and outer microbial platform and local slope in the southeast) (Woo, 2009). The local slope in the southeast triggered dilute density (turbidity) currents, forming sporadic normally graded calcarenite with load and flame structures. With recovery of carbonate factories, more carbonate sediments deposited under relatively shallow waters, forming an interval of thin-bedded limestone facies association (FA2) (Fig. 13b). The extensive deformed limestones resulted from differential deformation processes (brecciation, liquefaction/fluidization, and injection), most likely caused by pore-water overpressure during the period of rapid sea-level fall (Spence and Tucker, 1997; Chen et al., 2011).

5.2. Bounding Surface 2 and Sequence 2

5.2.1. Description

Surface 2 is characterized by an irregular, sharp surface with erosion relief up to 20 cm in height (Fig. 9). The erosion surface truncates the underlying strongly deformed, shallow-subtidal deposit. It contains the *Neodrepanura* Zone (Figs. 9 and 10). The erosion surface is overlain by sporadic microbial buildups (composed mainly of micrite, fossil fragments, and a few glauconite grains) and a relatively thick (0.6 to 4.5 m in thickness) *Chuangia*-bearing bioclastic grainstone (mainly containing trilobite fragments, brachiopod shells, and abundant glauconite grains) of the sequence 2 (Figs. 9 and 10). The *Prochuangia* Zone (between the *Neodrepanura* and *Chuangia* zones) is absent, although it occurs in Liaoning Province (China) and the Taebaek area (Korea). The geochemical data indicate an abrupt increase in carbon isotope value across the boundary, a large positive $\delta^{13}C$ excursion (Fig. 10). The bioclastic grainstone is successively overlain by a shale-dominated facies (FA1) (Fig. 10). The upper part of the sequence 2 contains a coarsening-upward succession with a thin-bedded limestone facies association (FA2) in the lower part and a thick (10–20 m) microbialite facies association (FA4) in the upper part (Fig. 7). The FA2 consists mainly of thin-bedded lime mudstone with shale or marlstone (facies L-S, L-M, and Ltb), limestone breccia and conglomerate (facies LB and LC), stratified grainstone (facies Gptc), and microbialite (facies

Table 2. Description and interpretation of facies associations

Facies association (FA)	Description	Interpretation
FA1: Shale-dominated facies association	Dominated by greenish-gray (yellowish-gray) shale (facies Sh), frequently intercalated with thin homogeneous lime mudstone beds, forming limestone-shale alternation (facies L-S); limestone-shale alternation commonly changing into discontinuous limestone breccia (facies LB); dm- to m-scale cycles comprising facies L-S in the lower part and facies Sh in the upper part; a few calcarenite (facies CA) beds with normal grading and small-scale load and flame structures.	Deposited in a low-energy, deep-water setting, most likely below storm-wave base (e.g., deep-subtidal environment) (Markello and Read, 1981; Glumac and Walker, 2000; Elrick and Snider, 2002).
FA2: Thin-bedded limestone facies association	Dominated by thin-bedded limestone facies, with a predominance of limestone-shale/marlstone alternation and thin-bedded lime mudstone (facies L-S/M and Ltb) in the lower part, and laminated calcisiltite, planar and trough cross-stratified grainstone, and stratified limestone conglomerate (facies Cl, Gptc, and LC) in the upper part; Facies L-S and L-M gradually changing into Ltb upward, forming dm- to m-scale cycles, overlain by facies LC with sharp boundaries; a few microbialite (facies Mtm) locally.	Formed in relatively shallow-water environments often affected by storm-induced distal currents (e.g., shallow-subtidal setting) (cf. Burchette and Wright, 1992; Kwon et al., 2006).
FA3: Grainstone facies association	Dominated by various grainstone facies such as planar or trough cross-stratified, crudely wavy-stratified, hummocky and swaley cross-stratified, or normally graded grainstones (facies Gptc, Gcw, Ghsc, and Gng); composed of fragmentary bioclasts, ooids, peloids, intraclasts, and abundant glauconite grains; limestone breccia and conglomerate, laminated calcisiltite, and limestone-shale alternation (facies LB, LC, Cl, and L-S) intercalated.	Formed in a storm-dominated carbonate shoreface/shoal near the normal wave base (Jiang et al., 2002, 2003; Betzler et al., 2007; Palma et al., 2007).
FA4: Microbialite facies association	Characterized by biostromal microbialite, with either flat-bedded or domal megastructures; including tabular maceriate (facies Mtm), columnar maceriate (facies Mcm), and columnar chaotic microbialite (facies Mcc); microbialite (up to 18 m in thickness) comprising several beds (up to 3 m thick), either interrupted by sharp internal boundaries or intercalated with non-microbial carbonate sediments; overlain by various types of grainstones of the FA3 with an irregular, sharp boundary.	Deposited on broad and relatively flat seafloor, forming an extensive subtidal microbialite flat (Grotzinger, 1986; James and Bourque, 1992; Lee et al., 2010).
FA5: Wackestone to grainstone facies association	Dominated by bioturbated lime mudstone to wackestone and wackestone to grainstone (facies Wb and W-G); thin layers (up to a few dm in thickness) of massive, normally graded, or stratified grainstone and limestone conglomerate, and limestone-shale alternation (facies Gng, Gcw, Gptc, LC, and L-S) partly interbedded; columnar stromatolite (facies Sc) (up to 11 m thick) locally present; bioturbated lime mudstone with U-shaped burrows, and rare occurrence of bi-directional wavy and lenticular bedded calcisiltite and lime mudstone breccia in the uppermost part.	Formed in a generally low-energy, restricted platform interior (or a wide, shallow lagoon) with intermittent high-energy conditions (cf. Osleger and Montañez, 1996; Nakazawa et al., 2009).

Mtm). The thick microbialite (FA4) consists of several flat-bedded units, which can be well correlated among the sections for tens of kilometers (Figs. 11 and 12).

5.2.2. Interpretation

Surface 2 is a cryptic subaerial unconformity, which lacks clear evidence for subaerial exposure such as desiccation cracks, fenestrae cavities, root casts, evaporite pseudomorphs, microbial laminites, paleosols, and paleokarsts. It nevertheless represents a significant subaerial hiatus which is reflected by the truncation of well-lithified deformed sediments, the missing of a trilobite biozone (*Prochuangia*), and the abrupt increase in carbon isotope value in the rising limb of a positive $\delta^{13}C$ excursion that can be globally correlated (i.e., the Steptoean positive carbon isotope excursion, SPICE) (Saltzman et al., 2000; Zhu et al., 2004; Chen et al., 2011) (Fig. 10). The sporadic microbial buildups on the topographic highs of the erosion surface indicate the first resurgence of the microbialites on the submerged seafloor. The microbial buildups were then buried by reworked fossil fragments, which formed a shoreface lag deposit during the period of low sedimentation rate as base level kept rising (Fig. 13d). The overlying shale-dominated facies association (FA1) indicates that the grainstone shoreface was drowned with rapid rise in base level (Figs. 7, 10, and 13e). As base-level rise slowed, a thin-bedded limestone facies association formed with a few beds of dm- to m-scale, biohermal, and m-scale, biostromal microbialite, indicating a gradual growth of microbialites in a shallow-subtidal setting (Fig. 13e). The microbialite eventually flourished and filled most accommodation, forming an extensive shallow-subtidal microbial flat (Fig. 13f).

5.3. Bounding Surface 3 and Sequence 3

5.3.1. Description

Surface 3 is represented by an abrupt shift from the flat-bedded microbialite below to the domal microbialite (or

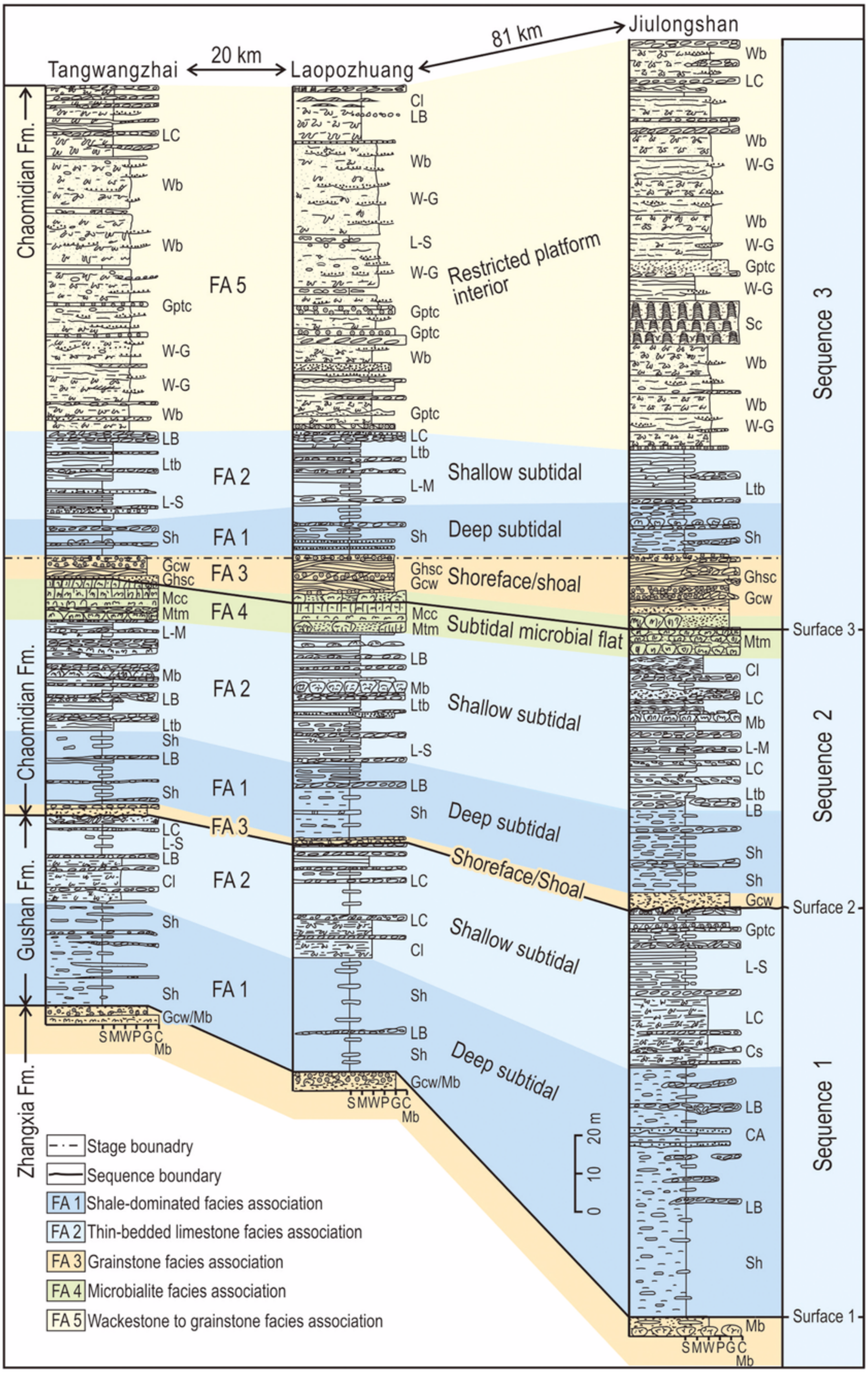

Fig. 7. Facies associations and depositional units of the major sections (for location, see Fig. 1c; for facies codes, see Table 1).

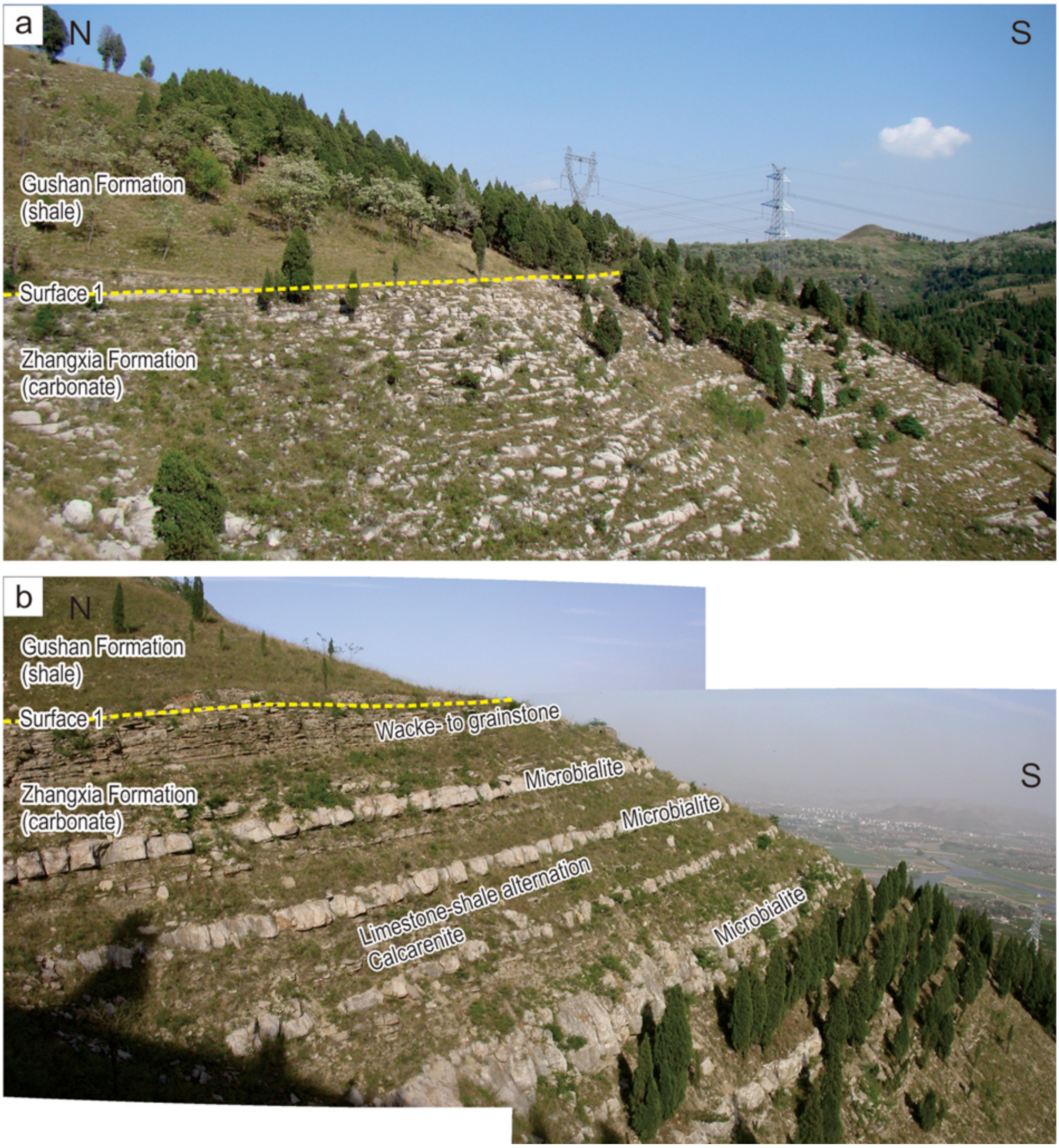

Fig. 8. Surface 1, a drowning surface that separates the underlying carbonates in the Zhangxia Formation and the overlying shales in the Gushan Formation. (a) Tangwangzhai section. (b) Jiulongshan section.

grainstone) above (Figs. 11 and 12). The underlying flat-bedded microbialites consist mainly of columnar microbialites (facies Mcm and Mcc) with minor non-microbial carbonate sediment. The surface is overlain by various deposit of sequence 3. It is either domal microbialite containing abundant dolomitic marlstone (Chengouwan section) or maceriate microbialite with abundant, laterally associated non-microbial carbonate sediments (e.g., fossil fragments, peloids, and intraclasts) (Jiulongshan section) (Figs. 11 and 12). The domal microbialite is overlain by grainstone-dominated facies (FA3) with an irregular surface (Fig. 11). The surface partly truncates the flat-bedded microbialite with erosion relief up to 2 m (Fig. 11b). The grainstone is overlain by thin shale-dominated facies (FA1) and thin-bedded limestone facies (FA2) (Fig. 7). The upper part of the sequence 3 is characterized by a monotonous succession of mainly bioturbated wackestone to grainstone (facies Wb and W-G) with a small portion of limestone-shale/marlstone alterna-

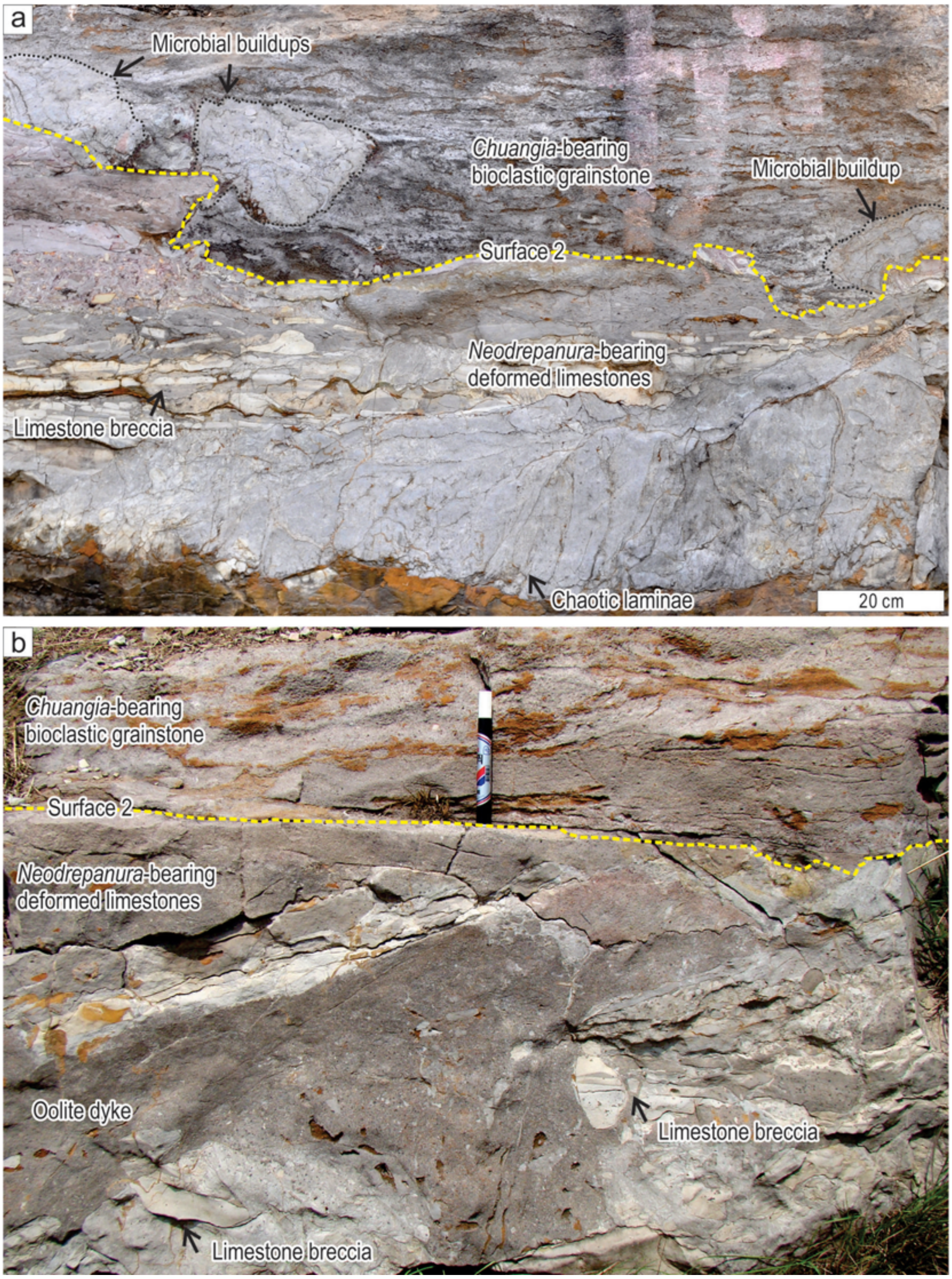

Fig. 9. Surface 2, a cryptic subaerial unconformity. (a) Surface 2 truncates deformed limestone bed and underlies sporadic microbial buildups and *Chuangia*-bearing bioclastic grainstone (Wanliangyu section). Scale bar is 10 cm long. (b) Surface 2 truncates strongly deformed limestone bed and underlies *Chuangia*-bearing bioclastic grainstone (Tangwangzhai section). Marker pen is 14.5 cm long.

tion (facies L-S/M), stratified grainstone (facies Gptc and Gcw), limestone conglomerate (facies LC), and stromatolite (facies Sc) (Fig. 7). A relatively thick (up to 11 m) stromatolite occurs in the Jiulongshan section (Fig. 6). The uppermost part of the sequence 3 is characterized by bioturbated lime mudstone with U-shaped burrows, and rare occurrence of bi-directional calcisiltite and lime mudstone breccia (Fig. 7).

5.3.2. Interpretation

Surface 3 represents an abrupt shift from flat-bedded

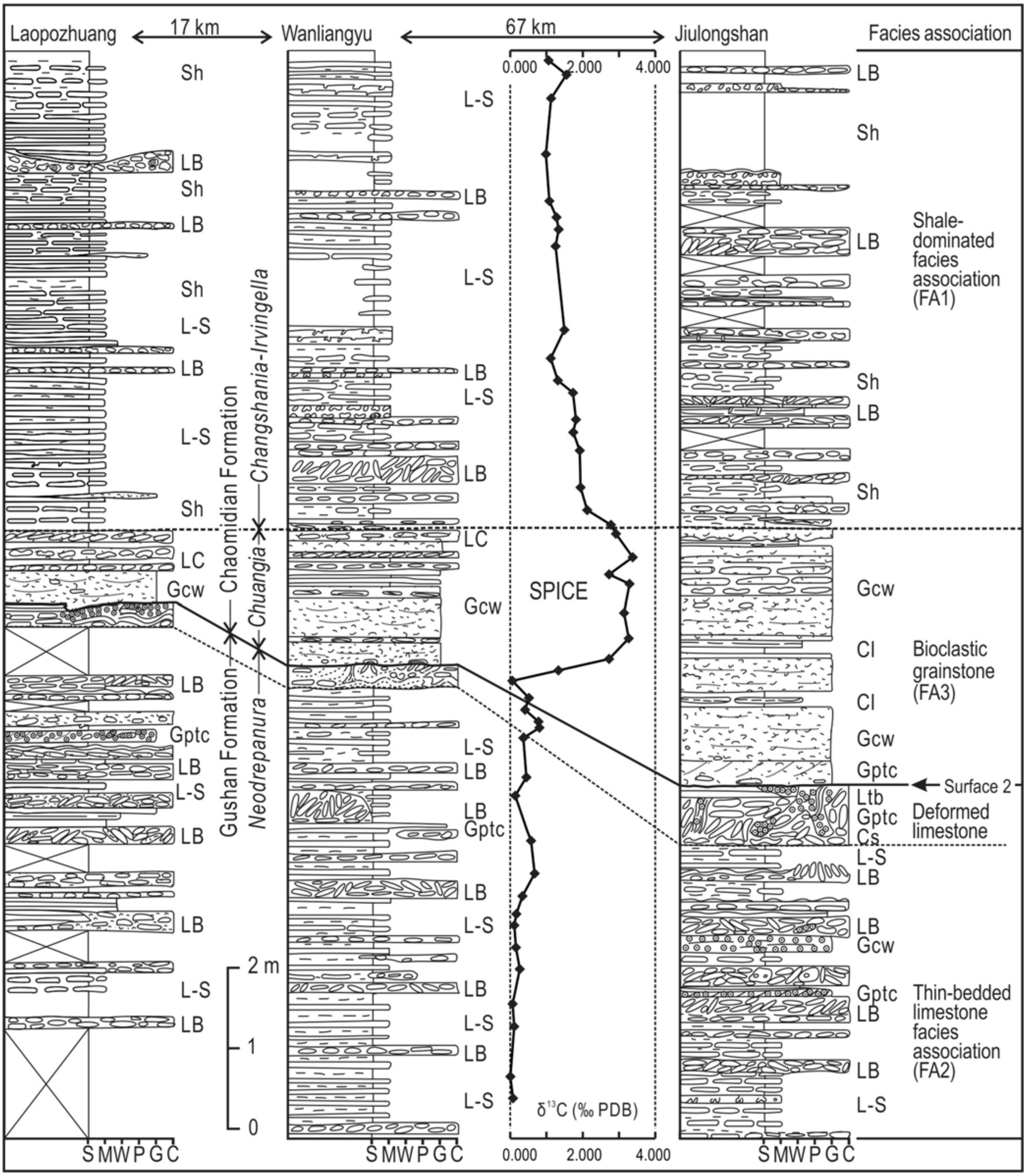

Fig. 10. Sedimentary logs showing the lateral traceability of surface 2 which truncates the underlying deformed limestone bed. Surface 2 is interpreted as a subaerial unconformity which is reflected by missing of a trilobite biozone (*Prochuangia* Zone) and abrupt increase in carbon isotopic value. SPICE: Steptoean positive carbon isotope excursion (Saltzman et al., 2000) (for facies code, see Table 1).

microbialite to domal microbialite (or grainstone). The surface, either 'hidden' in the thick microbialite or imprinted by submarine erosion, is indicative of a facies change during rapid rise in base level (Lee et al., 2012). During initial base-level rise, domal microbialite formed above the flooding surface in local topographic highs (e.g., Chengouwan

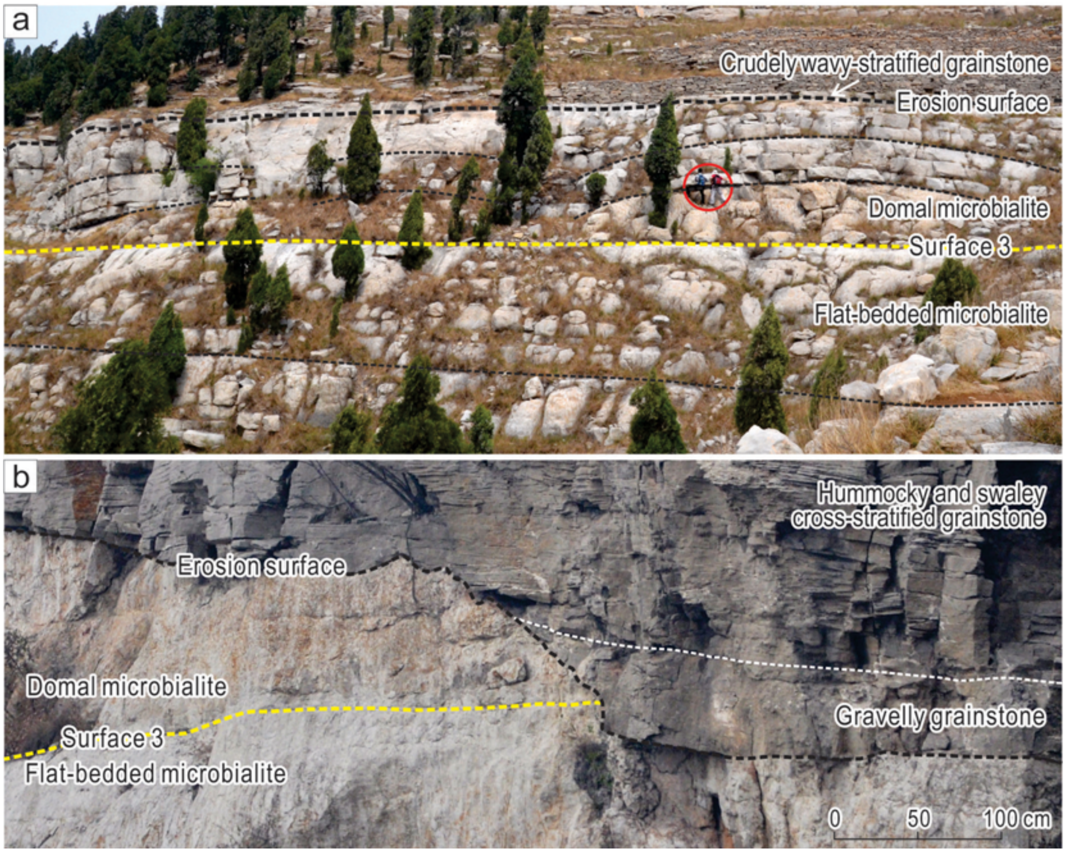

Fig. 11. Surface 3, a marine flooding surface. (a) Surface 3 is a distinct flat surface between the underlying flat-bedded microbialite and the overlying domal microbialite. The domal microbialite is overlain by grainstones with an erosion surface (Chengouwan section). (b) Surface 3 is partly imprinted by an erosion surface with significant relief (Tangwangzhai section).

section) due to catch-up ability under the conditions of increased accommodation (Fig. 13g). In the topographic lows, however, the microbialite could not catch up with base-level rise and were scoured by storm-induced waves and/or currents, forming a distinct erosion surface. They were then buried by coarse grainstone (Fig. 13g). The storm-dominated grainstone shoal/shoreface firstly developed in the southeast (e.g., Jiulongshan section) and caught up with the base-level rise, which resulted in the deposition of thick grainstone with abundant glauconites (FA3) (Kerans and Loucks, 2002). The grainstone shoal/shoreface aggraded and migrated to the northwest with ensued rise in base level, which finally terminated the microbialite in the Chengouwan section (Fig. 12). The grainstone shoal/shoreface was drowned with continued rise in base level, forming a shale-dominated facies association (FA1) (Figs. 12 and 13h). As the rate of base-level rise decreased, a thick highstand systems tract developed, including a relatively thin succession of thin-bedded limestone facies association (FA2) formed in a shallow-subtidal setting (Fig. 13h). A thick succession of bioturbated wackestone to grainstone (FA5) formed in a broad, generally low-energy restricted platform interior due to a balanced increase in accommodation and sediment supply (Bádenas and Aurell, 2008) (Fig. 13i). Local stromatolite patch reefs or barriers developed under favorable water conditions (e.g., depth, transparency, light, and nutrient) (Fig. 13i). The restricted area eventually changed into a shallow tidal flat, which was flooded again during the Early Ordovician (Meng et al., 1997).

6. INTRAPLATFORM CORRELATION

The Cambrian successions in both the Shandong region and the Taebaek area, Korea (eastern margin of the North China Platform, ca. 1,000 km east of the Shandong region) are generally correlated by trilobite faunal assemblages (Choi et al., 2003; Choi and Chough, 2005; Lee and Choi, 2007; Park et al., 2008; Chough et al., 2010; Park and Choi, 2011). The Teabaek area comprises a relatively thin (ca. 130 m in thickness) upper Cambrian Series 3 to Furongian succession of mixed carbonate and siliciclastic deposits (Sesong and Hwajeol formations) (Fig. 14). The Sesong Formation, overlying the carbonate-dominated Daegi Formation (mainly bioclastic wacke- to grainstone, oolite, and microbialite), is dominated by shale intercalated with lime mudstone and limestone breccia in the lower part and fine to

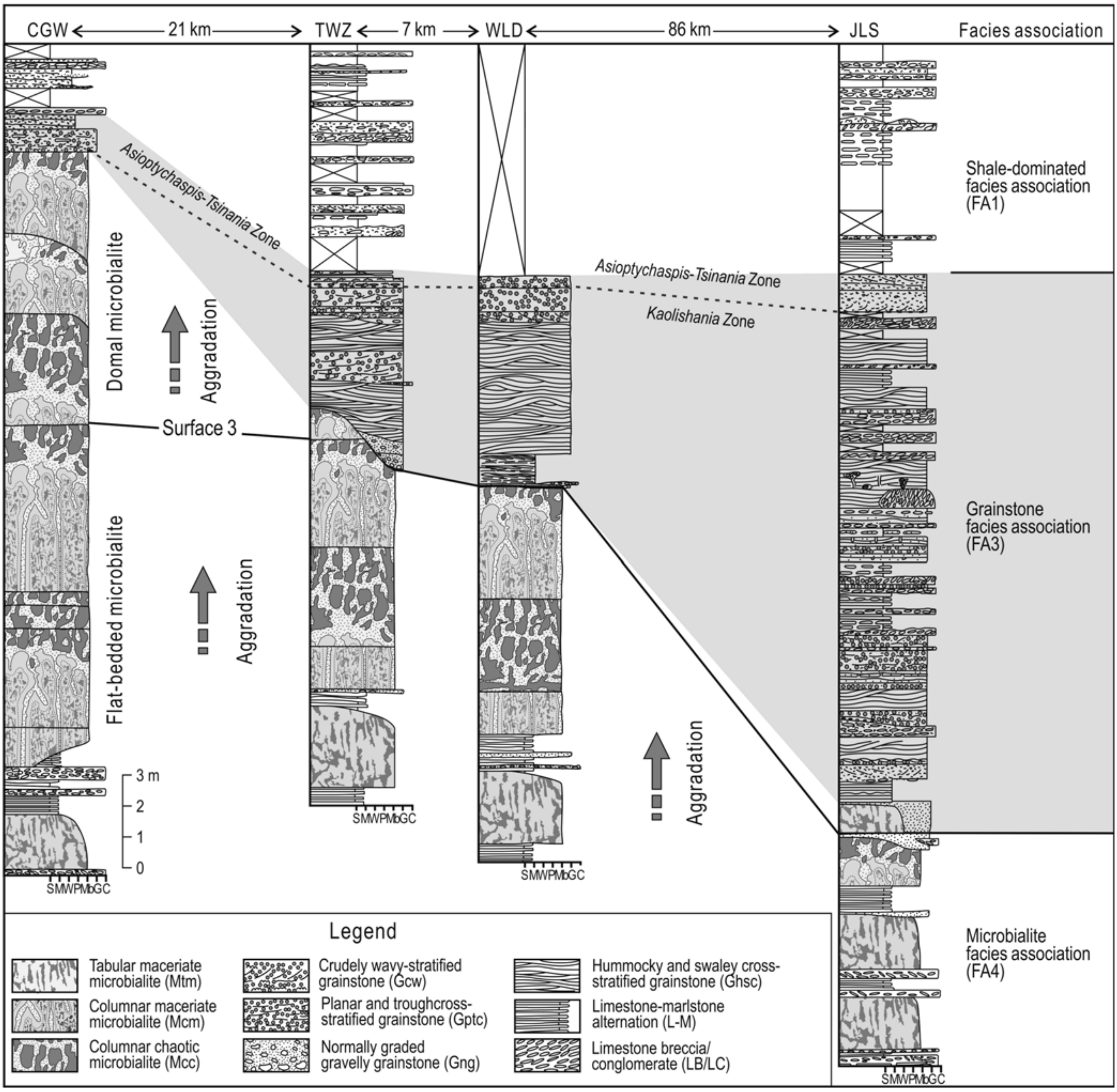

Fig. 12. Detailed sedimentary logs showing the characteristics of surface 3 (a flooding surface). Surface 3 is a distinct surface on top of the flat-bedded microbialite, which is overlain by either thick domal microbialite in the Chengouwan section (CGW) or thin microbialite (or non-microbial sediments) in the Tangwangzhai (TWZ), Wanglaoding (WLD), and Jiulongshan (JLS) sections.

medium sandstone in the upper part, interpreted as outer to inner shelf deposits (Kwon et al., 2006). The overlying Hwajeol Formation consists mainly of limestone-shale alternation, wacke- to grainstone, and limestone breccia, most likely deposited in outer to inner ramp (Kwon et al., 2006).

6.1. Correlation of Surface 1

A sequence (or supersequence) boundary of a drowning unconformity was identified between the Daegi and Sesong formations, which was correlated with surface 1 in the Shandong region (Kwon et al., 2006). Biostratigraphic correlation based on the occurrence of trilobite faunas indicates, however, that surface 1 formed much earlier in the Shandong region than that in the Taebaek area (Choi and Chough, 2005; Kang and Choi, 2007; Park et al., 2008, 2009; Chough et al., 2010; Park and Choi, 2011) (Fig. 14). The time discrepancy appears too large (approximately 1 m.y. gap by assuming that each biozone lasted about 1 m.y. on average) to be diachronous (Fig. 14). It could have thus resulted from

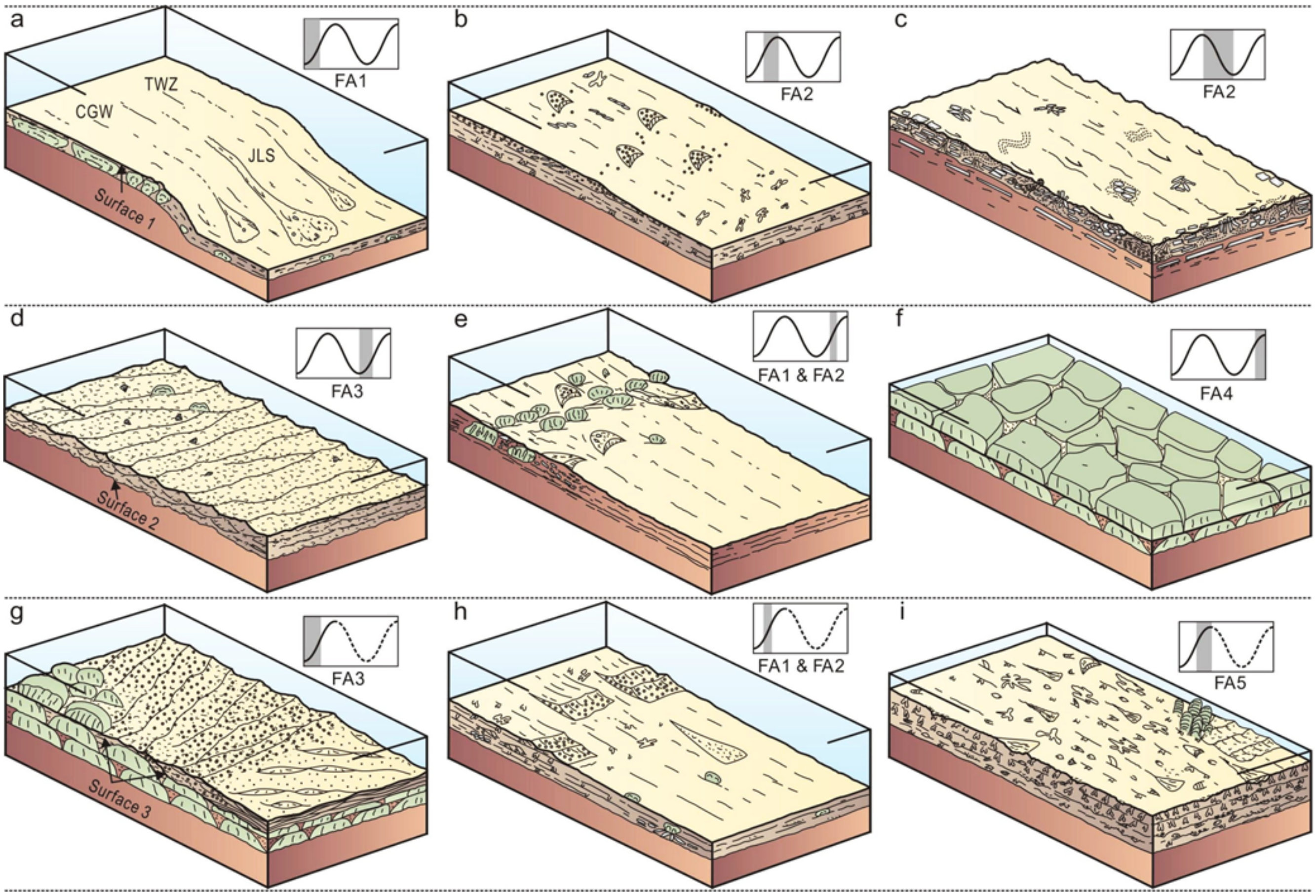

Fig. 13. Depositional model of the Gushan and Chaomidian formations (for facies association codes, see Table 2). (a) Drowning of the carbonate platform (Zhangxia Formation) with significant relief, forming a drowning surface (surface 1). (b) Progressive sedimentation of carbonates during highstand base level. (c) Subaerial exposure and erosion of a strongly deformed limestone bed, caused by rapid sea-level fall. (d) Resumed carbonate sedimentation upon the subaerial unconformity (surface 2) during base-level rise with the first occurrence of microbialite after drowning of the Zhangxia carbonate platform. (e) Gradual resurgence of microbialite during slowed rise in base level. (f) Flourish of microbialite during highstand base level. (g) Termination of flat-bedded microbialite by resumed rise in base level, forming a marine flooding surface (surface 3). Microbialite either resurged in the topographic highs or terminated by storm-induced erosion and subsequent deposition of grainstone in the topographic lows. (h) Progradation of carbonate sediments during the early stage of highstand base level. (i) Deposition of thick bioturbated wackestone during highstand base level of the epeiric carbonate platform. CGW: Chengouwan section, TWZ: Tangwangzhai section, JLS: Jiulongshan section.

an accumulated out-of-phase response to the base-level rise due to the original topographic relief and the difference in carbonate production rate as well as local depositional processes. During rapid rise in base level, carbonate factories were drowned and failed to catch up with base level rise in the topographic lows (Shandong region), forming a shale-dominated succession (FA1) above the surface 1 (Fig. 15a). In the topographic highs (Taebaek area), however, carbonate factories were re-established, catching up with the rising base level (Fig. 15a). The correlative flooding surface of surface 1 might have been 'hidden' in the carbonate deposit (Figs. 14 and 15a). The Taebaek area was eventually drowned by progressive rise in base level during the late Kushanian Age, whereas carbonate factories were gradually resurged contemporaneously in the Shandong region (Fig. 15b).

On the other hand, Sim and Lee (2006) postulated a sequence boundary of subaerial exposure in the middle part of the Daegi Formation based on obscure dissolution pipes and terra-rossa-like paleosols. However, detailed microfacies analysis indicates continuous prolific subaqueous sedimentation of various carbonates and negates the possibility of subaerial exposure (Hong et al., 2012). Meyerhoff et al. (1991) and Meng et al. (1997) suggested that diastrophism (epeirogenic tilting) occurred during late Cambrian Epoch 3 to early Furongian. However, the diastrophism was proposed merely based on large-scale lithological observations of some coeval strata across the North China Platform (e.g., shales in the northern part of the platform vs. dolomitized limestones in the southern part during the Kushanian Age)

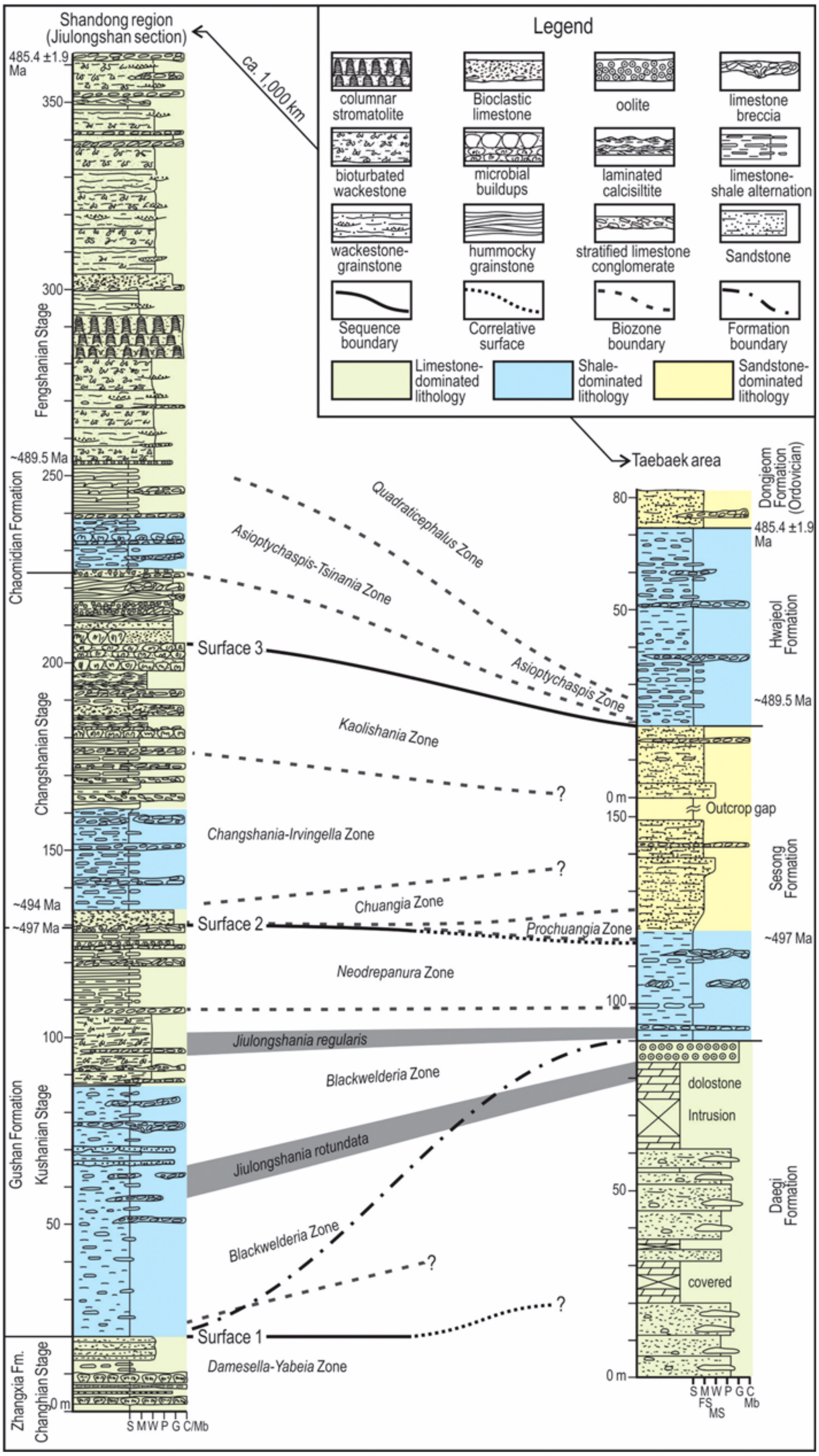

Fig. 14. Intraplatform correlation of the upper Cambrian Series 3 to Furongian succession in the North China Platform between the Shandong region (China) and the Taebaek area (Korea). The sedimentary column of the Taebaek area and the biostratigraphic data are from Choi and Chough (2005), Kwon et al. (2006), Kang and Choi (2007), Park et al. (2008, 2009), Chough et al. (2010), Park and Choi (2011), and Hong et al. (2012). S: shale, M: lime mudstone, W: wackestone, P: packstone, G: grainstone, C: limestone conglomerate, Mb: microbialite, FS: fine sandstone, MS: medium sandstone.

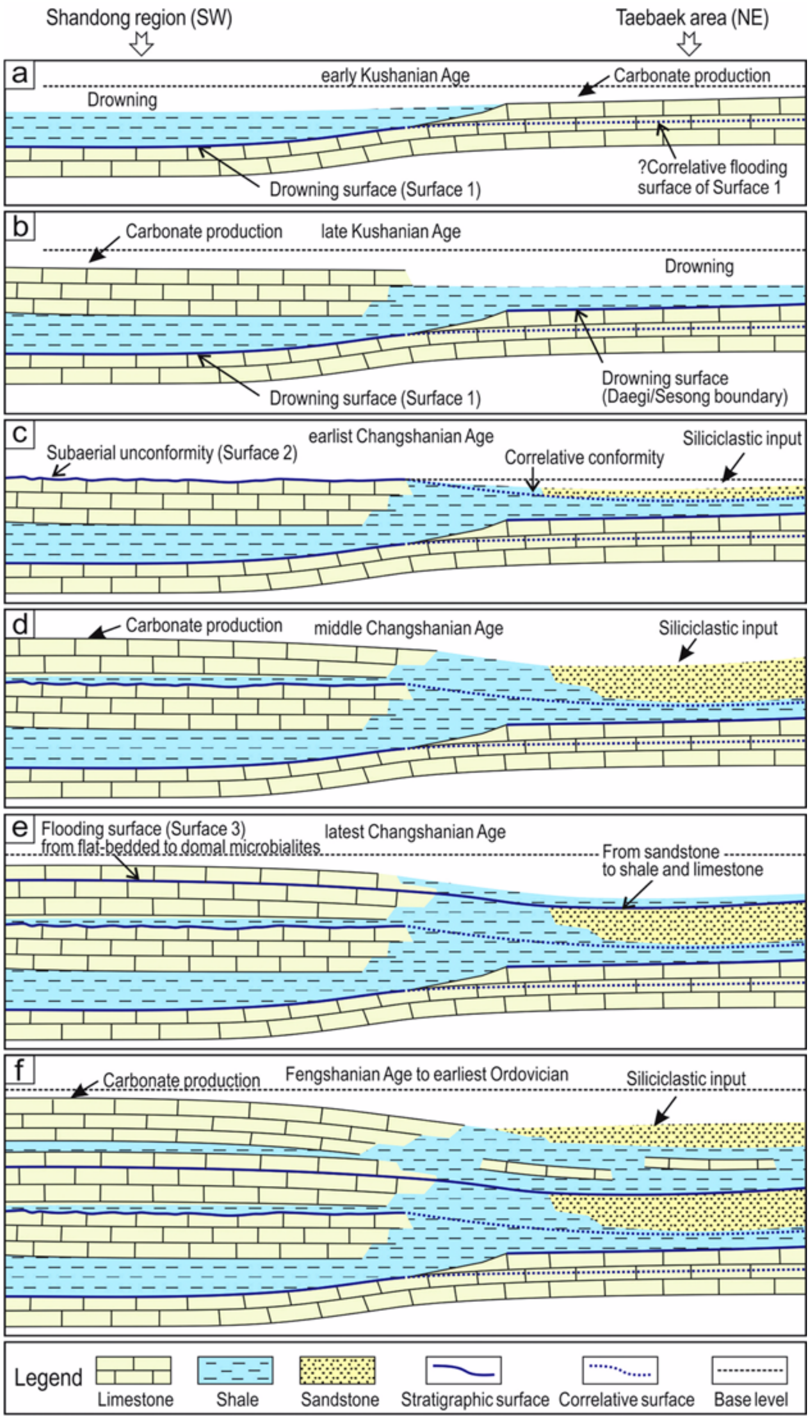

Fig. 15. Schematic models illustrating the formation of the stratigraphic surfaces. (a) Drowning of the middle Cambrian carbonate platform in the Shandong region during the early Kushanian Age, forming a drowning surface (surface 1). The relatively synchronous, correlative flooding surface would have been 'hidden' in the carbonate succession (Daegi Formation) in the Taebaek area. (b) During the late Kushanian Age, the Taebaek area was drowned by progressive base-level rise, forming a drowning surface; the carbonate factories gradually resurged in the Shandong region. (c) The Shandong region was subaerially exposed due to base level fall during the earliest Changshanian Age, resulting in the formation of a subaerial unconformity (surface 2). The Taebaek area continuously received siliciclastics, containing the *Prochuangia* Zone. (d) During the subsequent base-level rise and highstand during the middle to late Changshanian Age, the Shandong region was dominated by carbonate production, whereas siliciclastic input prevailed in the Taebaek area. (e) During the latest Changshanian Age, both regions were flooded again, forming a marine flooding surface (surface 3). It is represented by a shift of the flat-bedded microbialite to the domal microbialite in the Shandong region and from sandstones to nodular limestone and shale alternation in the Taebaek area. (f) Since the Fengshanian Age, carbonates prevailed in the Shandong region until the middle to late Ordovician, whereas deposition of shale and carbonate prevailed in the Taebaek area until the earliest Ordovician.

(Meng et al., 1997). In order to investigate the possibility of either large-scale diastrophism or regional/local variations in topography and sedimentary processes, more detailed sedimentary facies analyses are required in different locations of the entire North China Platform.

6.2. Correlation of Surface 2

The subaerial unconformity (i.e., surface 2) does not occur in the Taebaek area where the *Prochuangia* Zone is present (Park and Choi, 2011) (Fig. 14). The *Prochuangia* Zone occurs in a conformable, shale-dominated succession with gradual sedimentation of fine sandstones (Fig. 14). This suggests that the platform was subaerially exposed in the Shandong region but submerged in the Taebaek area. The discrepancy in the development of surface 2 in the two regions is ascribed to the topographic variations (Figs. 15a and b). During the period equivalent to the *Prochuangia* Zone, carbonate factories were shut down in the interior region of the platform (Shandong region) as a result of subaerial exposure (Fig. 15c). In the marginal region of the platform (Taebaek area), carbonate factories were constrained by siliciclastic sediment input which was most likely due to erosion of uplifted oldlands (cf. Kwon et al., 2006) (Fig. 15c). During the resumed rise in base level, carbonate factories were gradually recovered in the Shandong region during the middle Changshanian Age, whereas siliciclastic input was still dominant in the Taebaek area (Fig. 15d).

6.3. Correlation of Surface 3

A distinct surface, represented by an abrupt change in facies from the shallow-shelf sandstones in the upper part of the Sesong Formation to the outer-ramp limestone-shale alternations in the Hwajeol Formation, is recognized in the Taebaek area, indicating rapid rise in base level. The surface can be possibly correlated (with the aid of biostratigraphy) with the surface 3 (Fig. 14), only provided that both surfaces were formed by the same mechanism (i.e., same base-level rise). During rapid rise in base level at the latest Changshanian Age, the oldlands were submerged and siliciclastic input was shut down, resulting in the deposition of shales and carbonates in the Taebaek area (Fig. 15e). The correlative surface 3 is, however, 'hidden' in a carbonate-dominated succession in the Shandong region, reflected by abrupt change from the flat-bedded microbialites to the domal microbialites or grainstone-dominated deposits (Lee et al., 2012) (Figs. 11, 12, and 15e). After flooding, carbonate factories were recovered in the Shandong region and sedimentation was dominated by carbonates through the Ordovician. In the Taebaek area, deposition of shales and carbonates was dominated until the input of coarse-grained siliciclastic sediment, triggered again by another tectonic uplift during the earliest Ordovician (Kwon et al., 2006) (Fig. 15f).

7. DISCUSSION

The formation of high-frequency bounding surfaces is affected by diverse regional factors, which may result in high variability and low traceability depending on the differential influences. In addition to regional tectonics, sediment supply, and hydrodynamic conditions, topographic relief of the seafloor may significantly affect the development of stratigraphic sequences and their bounding surfaces. It results mainly from anteceded topography (e.g., basement), structural features (e.g., embayment and arch), and regional tectonics (subsidence, uplift, and tilting) (Rees, 1986; Christie-Blick and Driscoll, 1995; Meng et al., 1997; Myrow et al., 2003; Lee and Chough, 2011). In carbonate platforms, significant seafloor relief (e.g., marginal buildups, ooid shoals, and local slopes) may develop as a result of early marine cementation and different growth potential of carbonate factories (Kendall and Schlager, 1981; Burchette and Wright, 1992; Schlager, 1993; Burgess, 2001; Pomar, 2001; Woo, 2009). The regional topographic variations may lead to the high variability of high-frequency stratigraphic sequences and their bounding surfaces in carbonate systems.

During rapid rise in base level, a carbonate platform may be drowned as the deepened waters exceed the photic zone (i.e., an increase rate of accommodation exceeding that of sediment supply) and carbonate factories are shut down, forming a drowning surface (e.g., surface 1) (Schlager, 1989, 1999). However, the responses of the platform to rapid base-level rise may be different as a result of topographic variations: abrupt drowning of topographic lows and temporary catch-up of topographic highs. In cases of less rapid rise of base level, carbonate factories may be switched (e.g., from microbialite to grainstone) rather than drowned and new carbonate factories may catch up with the rising base level. Consequently, a relatively thick succession may form above a marine flooding surface (e.g., surface 3) during base-level rise (Kerans and Loucks, 2002). In both cases, the subtle stratigraphic surfaces may be partly 'hidden' within a carbonate-dominated succession, which are difficult to recognize and correlate in practice (Catuneanu, 2006).

As most accommodation is filled and water depth becomes very shallow during stillstand in base level, the topographic highs of the platform may be (partially) subaerially exposed during base-level fall, forming a subaerial unconformity (e.g., surface 2) (e.g., Osleger and Montañez, 1996). The topographic lows are not exposed and may continue to receive sediment, where the 'correlative conformity' is hardly recognized by its physical attributes, especially in the case of outcrop- or core-based studies. The correlative conformity is merely an imaginary surface that is correlated based on bio-chronostratigraphy. On exposed carbonate platforms, both subaerial erosion and chemical reworking give rise to the formation of desiccation cracks, karsts, dolomites, evaporites, fenestral cavities, or paleosols (Read and Grover, 1977; Hunt and Tucker, 1992; Osleger and Montañez, 1996; George and Chow, 1999; Schlager, 2004; Kwon et al., 2006; Catuneanu et al., 2009). The lack of these characteristics due to either lateral discontinuity or subsequent marine erosion, however, suggests that detailed facies analysis in combination with biostratigraphic and geochemical studies be required to examine the subaerial unconformity (Holland and Patzkowsky, 1998; Glumac and Spivak-Birndorf, 2002; Nakazawa et al., 2009; Chen et al., 2011; Glumac, 2011).

Furthermore, the high-frequency stratigraphic sequences and their bounding surfaces are not universally of eustatic origin; they can also be generated by changes in sediment supply and regional tectonics (Schlager, 1993; Christie-Blick and Driscoll, 1995; Miall, 1995; Burgess, 2001; Christie-Blick et al., 2007; Catuneanu et al., 2009; Miall, 2010). Moreover, the differentiation of eustatic vs. regional controls on their formation is hardly certain. The eustatic signal can be retarded or obscured by other variable controls (e.g., regional tectonics, siliciclastic supply, carbonate production, hydrodynamic conditions, sediment compaction and loading, and seafloor relief), which causes the diachronism or even disappearance of stratigraphic surfaces (Tipper, 1997; Pekar et al., 2001, 2003; Christie-Blick et al., 2007; Glumac and Mutti, 2007; Yoshida et al., 2007). It is for these reasons that high-frequency stratigraphic sequences and their bounding surfaces are invalid for correlation in a basin scale or among sedimentary basins worldwide.

8. CONCLUSIONS

The upper Cambrian Series 3 to Furongian Gushan and Chaomidian formations in Shandong Province, China consist mainly of carbonates with minor shales, which formed on an epeiric platform. The entire succession comprises three stratigraphic sequences, bounded at the base by a drowning surface (surface 1), a subaerial unconformity (surface 2), and a marine flooding surface (surface 3), respectively. Surface 1 is represented by an abrupt facies change from carbonates to the overlying shales. Surface 2 is indicated by an erosion surface on top of an extensive deformed limestone bed, missing of *Prochuangia* Zone, and an abrupt increase in carbon isotope value. Surface 3 is reflected by a subtle transition from flat-bedded microbialites to domal microbialites or grainstones. These surfaces are traced for about 6,000 km^2 in area in the Shandong region, but hardly correlated with the Taebaek area (about 1,000 km apart). The high variability of the bounding surfaces in the epeiric carbonate platform can be mainly ascribed to a complex interplay among differential carbonate production, siliciclastic input, hydrodynamic conditions, and topographic relief. It suggests that a regional bounding surface can be invalid for the sequence-stratigraphic correlation in a vast epeiric platform.

ACKNOWLEDGMENTS: This study was supported to SKC by the National Research Foundation of Korea (20110030964) and to ZH by the National Natural Science Foundation of China (40972043 and 41040018). We gratefully acknowledge D.K. Choi, T.-Y. Park, J. Woo, H.S. Lee, and S.-B. Lee for the helpful discussions in the field and laboratory. We thank two anonymous reviewers for their helpful comments on the manuscript.

REFERENCES

Adams, R.D. and Grotzinger, J., 1996, Lateral continuity of facies and parasequences in Middle Cambrian platform carbonates, Carrara Formation, southeastern California, U.S.A. Journal of Sedimentary Research, 66, 1079–1090.

Bádenas, B. and Aurell, M., 2008, Kimmeridgian epeiric sea deposits of northeast Spain: sedimentary dynamics of a storm-dominated carbonate ramp. In: Pratt, B.R. and Holmden, C. (eds.), Dynamics of Epeiric Seas, St. John's, 55–72.

Betzler, C., Pawellek, T., Abdullah, M., and Kossler, A., 2007, Facies and stratigraphic architecture of the Korallenoolith Formation in North Germany (Lauensteiner Pass, Ith Mountains). Sedimentary Geology, 194, 61–75.

Brandano, M. and Corda, L., 2002, Nutrients, sea level and tectonics: constrains for the facies architecture of a Miocene carbonate ramp in central Italy. Terra Nova, 14, 257–262.

Brett, C.E., Baird, G.C., Bartholomew, A.J., DeSantis, M.K., and Ver Straeten, C.A., 2011, Sequence stratigraphy and a revised sea-level curve for the Middle Devonian of eastern North America. Palaeogeography, Palaeoclimatology, Palaeoecology, 304, 21–53.

Burchette, T.P. and Wright, V.P., 1992, Carbonate ramp depositional systems. Sedimentary Geology, 79, 3–57.

Burgess, P.M., 2001, Modeling carbonate sequence development without relative sea-level oscillations. Geology, 29, 1127–1130.

Caron, V., Nelson, C.S., and Kamp, P.J.J., 2004, Transgressive surfaces of erosion as sequence boundary markers in cool-water shelf carbonates. Sedimentary Geology, 164, 179–189.

Catuneanu, O., 2006, Principles of sequence stratigraphy. Elsevier, Amsterdam, 375 p.

Catuneanu, O., Abreu, V., Bhattacharya, J.P., Blum, M.D., Dalrymple, R.W., Eriksson, P.G., Fielding, C.R., Fisher, W.L., Galloway, W.E., Gibling, M.R., Giles, K.A., Holbrook, J.M., Jordan, R., Kendall, C.G.S.C., Macurda, B., Martinsen, O.J., Miall, A.D., Neal, J.E., Nummedal, D., Pomar, L., Posamentier, H.W., Pratt, B.R., Sarg, J.F., Shanley, K.W., Steel, R.J., Strasser, A., Tucker, M.E., and Winker, C., 2009, Towards the standardization of sequence stratigraphy. Earth-Science Reviews, 92, 1–33.

Chen, J., Chough, S.K., Han, Z., and Lee, J.-H., 2011, An extensive erosion surface of a strongly deformed limestone bed in the Gushan and Chaomidian formations (late Middle Cambrian to Furongian), Shandong Province, China: Sequence–stratigraphic implications. Sedimentary Geology, 233, 129–149.

Choi, D.K., Kim, D.H., Sohn, J.W., and Lee, S.-B., 2003, Trilobite faunal successions across the Cambrian–Ordovician boundary intervals in Korea and their correlation with China and Australia. Journal of Asian Earth Sciences, 21, 781–793.

Choi, D.K. and Chough, S.K., 2005, The Cambrian-Ordovician stratigraphy of the Taebaeksan Basin, Korea: a review. Geosciences Journal, 9, 187–214.

Chough, S.K., Kwon, S.T., Ree, J.H., and Choi, D.K., 2000, Tectonic and sedimentary evolution of the Korean peninsula: a review and new view. Earth-Science Reviews, 52, 175–235.

Chough, S.K., Lee, H.S., Woo, J., Chen, J., Choi, D.K., Lee, S.-b., Kang, I., Park, T.-Y., and Han, Z., 2010, Cambrian stratigraphy of the North China Platform: revisiting principal sections in Shandong Province, China. Geosciences Journal, 14, 235–268.

Christie-Blick, N. and Driscoll, N.W., 1995, Sequence Stratigraphy. Annual Review of Earth and Planetary Sciences, 23, 451–478.

Christie-Blick, N., Pekar, S.F., and Madof, A.S., 2007, Is there a role for sequence stratigraphy in chronostratigraphy? Stratigraphy, 4, 217–229.

Dunham, R.J., 1962, Classification of carbonate rocks according to depositional texture. In: Ham, W.E. (ed.), Classification of Carbonate Rocks, Tulsa, 108–121.

Elrick, M. and Snider, A.C., 2002, Deep-water stratigraphic cyclicity and carbonate mud mound development in the Middle Cambrian Marjum Formation, House Range, Utah, USA. Sedimentology, 49, 1021–1047.

George, A.D. and Chow, N., 1999, Palaeokarst development in a lower Frasnian (Devonian) platform succession, Canning Basin, northwestern Australia. Australian Journal of Earth Sciences, 46, 905–913.

Glumac, B. and Walker, K.R., 2000, Carbonate deposition and sequence stratigraphy of the Terminal Cambrian Grand Cycle in the Southern Appalachians, U.S.A. Journal of Sedimentary Research, 70, 952–963.

Glumac, B. and Spivak-Birndorf, M.L., 2002, Stable isotopes of carbon as an invaluable stratigraphic tool: An example from the Cambrian of the northern Appalachians, USA. Geology, 30, 563–566.

Glumac, B. and Mutti, L.E., 2007, Late Cambrian (Steptoean) sedimentation and responses to sea-level change along the northeastern Laurentian margin: Insights from carbon isotope stratigraphy. GSA Bulletin, 119, 623–636.

Glumac, B., 2011, High-resolution stratigraphy and correlation of Cambrian strata using carbon isotopes: an example from the southern Appalachians, USA. Carbonates and Evaporites, 26, 287–297.

Grotzinger, J.P., 1986, Evolution of early Proterozoic passive-margin carbonate platform, Rocknest Formation, Wopmay Orogen, Northwest Territories, Canada. Journal of Sedimentary Petrology, 56, 831–847.

Holland, S.M. and Patzkowsky, M.E., 1998, Sequence stratigraphy and relative sea-level history of the Middle and Upper Ordovician of the Nashville Dome, Tennessee. Journal of Sedimentary Research, 68, 684–699.

Hong, J., Cho, S.-H., Choh, S.-J., Woo, J., and Lee, D.-J., 2012, Middle Cambrian siliceous sponge-calcimicrobe buildups (Daegi Formation, Korea): Metazoan buildup constituents in the aftermath of the Early Cambrian extinction event. Sedimentary Geology, 253–254, 47–57.

Hunt, D. and Tucker, M.E., 1992, Stranded parasequences and the forced regressive wedge systems tract: deposition during base-level fall. Sedimentary Geology, 81, 1–9.

James, N.P. and Bourque, P.-A., 1992, Reefs and mounds. In: Walker, R.G. and James, N.P. (eds.), Facies Models: Response to Sea Level Change, St. John's, 323–348.

Jiang, G., Christie-Blick, N., Kaufman, A.J., Banerjee, D.M., and Rai, V., 2002, Sequence stratigraphy of the Neoproterozoic Infra Krol Formation and Krol Group, Lesser Himalaya, India. Journal of Sedimentary Research, 72, 524–542.

Jiang, G., Christie-Blick, N., Kaufman, A.J., Banerjee, D.M., and Rai, V., 2003, Carbonate platform growth and cyclicity at a terminal Proterozoic passive margin, Infra Krol Formation and Krol Group, Lesser Himalaya, India. Sedimentology, 50, 921–952.

Kang, I. and Choi, D., 2007, Middle cambrian trilobites and biostratigraphy of the daegi formation (Taebaek Group) in the Seokgaejae section, Taebaeksan Basin, Korea. Geosciences Journal, 11, 279–296.

Kendall, C.G.S. and Schlager, W., 1981, Carbonates and relative changes in sea level. Marine Geology, 44, 181–212.

Kerans, C. and Loucks, R.G., 2002, Stratigraphic setting and controls on occurrence of highenergy carbonate beach deposits: Lower Cretaceous of the Gulf of Mexico. Gulf Coast Association of Geological Societies Transactions, 52, 517–526.

Kwon, Y.K., Chough, S.K., Choi, D.K., and Lee, D.J., 2006, Sequence stratigraphy of the Taebaek Group (Cambrian–Ordovician), mideast Korea. Sedimentary Geology, 192, 19–55.

Lee, H.S. and Chough, S.K., 2006, Lithostratigraphy and depositional environments of the Pyeongan Supergroup (Carboniferous–Permian) in the Taebaek area, mid-east Korea. Journal of Asian Earth Sciences, 26, 339–352.

Lee, H.S. and Chough, S.K., 2011, Depositional processes of the Zhushadong and Mantou formations (Early to Middle Cambrian), Shandong Province, China: roles of archipelago and mixed carbonate-siliciclastic sedimentation on cycle genesis during initial flooding of the North China Platform. Sedimentology, 58, 1530–1572.

Lee, J.-H., Chen, J., and Chough, S.K., 2010, Paleoenvironmental implications of an extensive maceriate microbialite bed in the Furongian Chaomidian Formation, Shandong Province, China. Palaeogeography, Palaeoclimatology, Palaeoecology, 297, 621–632.

Lee, J.-H., Chen, J., and Chough, S.K., 2012, Demise of an extensive biostromal microbialite in the Furongian (late Cambrian) Chaomidian Formation, Shandong Province, China. Geosciences Journal, 16, 275–287.

Lee, S.-B. and Choi, D.K., 2007, Trilobites of the Pseudokoldinioidia Fauna (Uppermost Cambrian) from the Taebaek Group, Taebaeksan Basin, Korea. Journal of Paleontology, 81, 1454–1465.

Markello, J.R. and Read, J.F., 1981, Carbonate ramp-to-deeper shale shelf transitions of an Upper Cambrian intrashelf basin, Nolichucky Formation, Southwest Virginia Appalachians. Sedimentology, 28, 573–597.

Mateu-Vicens, G., Pomar, L., and Tropeano, M., 2008, Architectural complexity of a carbonate transgressive systems tract induced by basement physiography. Sedimentology, 55, 1815–1848.

McKenzie, N.R., Hughes, N.C., Myrow, P.M., Choi, D.K., and Park, T.y., 2011, Trilobites and zircons link north China with the eastern Himalaya during the Cambrian. Geology, 39, 591–594.

Meng, X., Ge, M., and Tucker, M.E., 1997, Sequence stratigraphy, sea-level changes and depositional systems in the Cambro-Ordovician of the North China carbonate platform. Sedimentary Geology, 114, 189–222.

Meyerhoff, A.A., Kamen-Kaye, M., Chen, C., and Taner, I., 1991, China – Stratigraphy, Paleogeography, and Tectonics. Kluwer Academic Publishers, Dordrecht, 188 p.

Miall, A.D., 1995, Whither stratigraphy? Sedimentary Geology, 100, 5–20.

Miall, A.D., 2010, The Geology of Stratigraphic Sequences - 2nd Ed. Springer, New York, Heidelberg, 522 p.

Myrow, P.M., Taylor, J.F., Miller, J.F., Ethington, R.L., Ripperdan, R.L., and Allen, J., 2003, Fallen arches: Dispelling myths concerning Cambrian and Ordovician paleogeography of the Rocky Mountain region. GSA Bulletin, 115, 695–713.

Nakazawa, T., Ueno, K., Kawahata, H., Fujikawa, M., and Kashiwagi, K., 2009, Facies stacking patterns in high-frequency sequences

influenced by long-term sea-level change on a Permian Panthalassan oceanic atoll: An example from the Akiyoshi Limestone, SW Japan. Sedimentary Geology, 214, 35–48.
Osleger, D. and Montañez, I.P., 1996, Cross-platform architecture of a sequence boundary in mixed siliciclastic-carbonate lithofacies, Middle Cambrian, southern Great Basin, USA. Sedimentology, 43, 197–217.
Palma, R.M., López-Gómez, J., and Piethé, R.D., 2007, Oxfordian ramp system (La Manga Formation) in the Bardas Blancas area (Mendoza Province) Neuquén Basin, Argentina: Facies and depositional sequences. Sedimentary Geology, 195, 113–134.
Park, T.-Y., Han, Z., Bai, Z., and Choi, D., 2008, Two middle Cambrian trilobite genera, *Cyclolorenzella* Kobayashi, 1960 and *Jiulongshania* gen. nov., from Korea and China. Alcheringa, 32, 247–269.
Park, T.-Y., Kim, J.-H., and Choi, D.K., 2009, A middle Cambrian trilobite fauna from the lowermost part of the Sesong Formation at Gadeoksan, northern part of Taebaek. Journal of Paleontological Society of Korea, 25, 119-128. (in Korean with English abstract).
Park, T.-Y. and Choi, D.K., 2011, Trilobite faunal successions across the base of the Furongian Series in the Taebaek Group, Taebaeksan Basin, Korea. Geobios, 44, 481–498.
Pekar, S.F., Christie-Blick, N., Kominz, M.A., and Miller, K.G., 2001, Evaluating the stratigraphic response to eustasy from Oligocene strata in New Jersey. Geology, 29, 55–58.
Pekar, S.F., Christie-Blick, N., Miller, K.G., and Kominz, M.A., 2003, Quantitative constraints on the origin of stratigraphic architecture at passive continental margins: Oligocene sedimentation in New Jersey, U.S.A. Journal of Sedimentary Research, 73, 227–245.
Pomar, L., 2001, Types of carbonate platforms: a genetic approach. Basin Research, 13, 313–334.
Pomar, L. and Kendall, C.G.S.C., 2008, Architecture of carbonate platforms: A response to hydrodynamics and evolving ecology. In: Lukasik, J.J. and Simo, J.A. (eds.), Controls on Carbonate Platform and Reef Development, Tulsa, 187–216.
Read, J.F. and Grover, G.A., 1977, Scalloped and planar erosional surfaces, Middle Ordovician limestones, Virginia: analogues of Holocene exposed karst or tidal rock platforms. Journal of Sedimentary Petrology, 47, 956–972.
Rees, M.N., 1986, A fault-controlled trough through a carbonate platform: The Middle Cambrian House Range embayment. GSA Bulletin, 97, 1054–1069.
Saltzman, M.R., Ripperdan, R.L., Brasier, M.D., Lohmann, K.C., Robison, R.A., Chang, W.T., Peng, S., Ergaliev, E.K., and Runnegar, B., 2000, A global carbon isotope excursion (SPICE) during the Late Cambrian: relation to trilobite extinctions, organic-matter burial and sea level. Palaeogeography, Palaeoclimatology, Palaeoecology, 162, 211–223.
Schlager, W., 1989, Drowning unconformities on carbonate platforms. In: Crevello, P.D., Wilson, J.L., Sarg, J.F., and Read, J.F. (eds.), Controls on Carbonate Platform and Basin Development, Tulsa, 15–25.
Schlager, W., 1993, Accommodation and supply – a dual control on stratigraphic sequences. Sedimentary Geology, 86, 111–136.
Schlager, W., 1999, Type 3 sequence boundaries. In: Harris, P.M., Saller, A.H., and Simo, J.A. (eds.), Advances in Carbonate Sequence Stratigraphy: Application to Reservoirs, Outcrops, and Models, Tulsa, 35–46.
Schlager, W., 2004, Fractal nature of stratigraphic sequences. Geology, 32, 185–188.
Schlager, W., 2005, Carbonate Sedimentology and Sequence Stratigraphy. SEPM, Concepts in Sedimentology and Paleontology Series 8, Amsterdam, 200 p.
Scotese, C.R. and McKerrow, W.S., 1990, Revised World maps and introduction. Geological Society of London Memoirs, 12, 1–21.
Sim, M. and Lee, Y., 2006, Sequence stratigraphy of the Middle Cambrian Daegi Formation (Korea), and its bearing on the regional stratigraphic correlation. Sedimentary Geology, 191, 151–169.
Spence, G.H. and Tucker, M.E., 1997, Genesis of limestone megabreccias and their significance in carbonate sequence stratigraphic models: a review. Sedimentary Geology, 112, 163–193.
Strasser, A., Pittet, B., Hillgartner, H., and Pasquier, J.-B., 1999, Depositional sequences in shallow carbonate-dominated sedimentary systems: concepts for a high-resolution analysis. Sedimentary Geology, 128, 201–221.
Tipper, J.C., 1997, Modeling carbonate platform sedimentation—Lag comes naturally. Geology, 25, 495–498.
Woo, J., 2009, The Middle Cambrian Zhangxia Formation, Shandong Province, China: Depositional Environments and Microbial Sedimentation. Ph.D. Thesis, Seoul National University, Seoul, South Korea, 243 p.
Yoshida, S., Steel, R., and Dalrymple, R., 2007, Changes in depositional processe—an ingredient in a new generation of sequence-stratigraphic models. Journal of Sedimentary Research, 77, 447–460.
Zhang, Z., Zhang, S., Song, Z., and Chi, S., 1994, Suggestions on the division and correlation of the Cambrian-Early Ordovician stratigraphy in Shandong Province. Shandong Geology, 10, 28–39. (in Chinese with English abstract).
Zhu, M.-Y., Zhang, J.-M., Li, G.-X., and Yang, A.-H., 2004, Evolution of C isotopes in the Cambrian of China: implications for Cambrian subdivision and trilobite mass extinctions. Geobios, 37, 287–301.

Manuscript received March 1, 2012
Manuscript accepted October 17, 2012